AD_____

Award Number: W81XWH-07-1-0193

TITLE: Spring Ankle with Regenerative Kinetics to Build a New Generation of Transtibial Prostheses

PRINCIPAL INVESTIGATOR:Dr. Thomas Sugar, PhD, PE

CONTRACTING ORGANIZATION:
Arizona State University

Tempe, AZ 85287-3503

REPORT DATE: July 2009

TYPE OF REPORT: Annual

PREPARED FOR: U.S. Army Medical Research and Materiel Command
Fort Detrick, Maryland 21702-5012

DISTRIBUTION STATEMENT:

x Approved for public release; distribution unlimited

REPORT DOCUMENTATION PAGE

Form Approved
OMB No. 0704-0188

1. REPORT DATE *(DD-MM-YYYY)*	**2. REPORT TYPE**	**3. DATES COVERED** *(From - To)*
01-07-2009	Annual	1 Aug 2008 – 31 July 2009

4. TITLE AND SUBTITLE
Spring Ankle with Regenerative Kinetics to Build a New Generation of Transtibial Prostheses.

5a. CONTRACT NUMBER

5b. GRANT NUMBER
W81XWH-07-1-0193

5c. PROGRAM ELEMENT NUMBER

6. AUTHOR(S)
Dr. Thomas G. Sugar

5d. PROJECT NUMBER

5e. TASK NUMBER

5f. WORK UNIT NUMBER

7. PERFORMING ORGANIZATION NAME(S) AND ADDRESS(ES)
Arizona State University

Tempe AZ 85287-3503

8. PERFORMING ORGANIZATION REPORT NUMBER

9. SPONSORING / MONITORING AGENCY NAME(S) AND ADDRESS(ES)
US Army Medical Research and Materiel Command
Fort Detrick, MD 21702-5012

10. SPONSOR/MONITOR'S ACRONYM(S)

11. SPONSOR/MONITOR'S REPORT NUMBER(S)

12. DISTRIBUTION / AVAILABILITY STATEMENT
Approved for public release

13. SUPPLEMENTARY NOTES

14. ABSTRACT

The goal is to design the *Spring Ankle with Regenerative Kinetics (SPARKy)* which seeks to develop a new generation of powered prosthetic devices based on the Robotic Tendon actuator. This actuator is a lightweight motor and transmission in series with a helical spring that significantly minimizes the peak power requirement of an electric motor and total system energy. The Robotic Tendon has kinetic advantages and stores and releases energy to provide SPARKy users with 100% of required push-off power and ankle range of motion comparable to able-bodied ankle motion while maintaining a form factor that is portable to the wearer.

In the second year, we developed and tested a transtibial prosthesis that supports continuous unstructured walking for up to 2.8 hours. A pilot study with 2 subjects tested the device. An independent gait laboratory will compare gait symmetry and metabolic consumption of SPARKy versus the subject's conventional prostheses. All components are worn and are lightweight and portable.

15. SUBJECT TERMS
Transtibial Prosthesis, regenerative, spring, wearable robot

16. SECURITY CLASSIFICATION OF:			**17. LIMITATION OF ABSTRACT**	**18. NUMBER OF PAGES**	**19a. NAME OF RESPONSIBLE PERSON**
a. REPORT	**b. ABSTRACT**	**c. THIS PAGE**			USAMRMC
U	U	U	UU	51	**19b. TELEPHONE NUMBER** *(include area code)*

Standard Form 298 (Rev. 8-98)
Prescribed by ANSI Std. Z39.18

Table of Contents

Introduction

"SPARKy – Spring Ankle with Regenerative Kinetics" to build a new generation of transtibial prostheses

Keywords: Transtibial Prosthesis, regenerative, spring, wearable robot

The goal is to design the *Spring Ankle with Regenerative Kinetics (SPARKy)* which seeks to develop a new generation of powered prosthetic devices based on the Robotic Tendon actuator. This actuator is a lightweight motor and transmission in series with a helical spring that significantly minimizes the peak power requirement of an electric motor and total system energy. The Robotic Tendon has kinetic advantages and stores and releases energy to provide SPARKy users with 100% of required push-off power and ankle range of motion comparable to able-bodied ankle motion while maintaining a form factor that is portable to the wearer.

Objective: The SPARKy Team using several unique technologies developed at Arizona State University's Human Machine Integration Lab will build a new generation of smart, active, energy-storing, transtibial prostheses that will support a Military amputee's return to active duty.

Military Relevance: Military amputees have unique requirements not found in the general amputee population. Military amputees are typically highly active and young. Their profession requires that they perform physically demanding dynamic tasks under severe conditions. Current state-of-the-art devices that are commercially available and in research do not address their unique requirements. SPARKy is the only device of its kind designed to address the technologically challenging requirements of the highly active Military amputees. SPARKy is very powerful and efficient. This will allow the amputee to carry heavy loads while walking at speeds up to 2 m/s. The mechanical design addresses the demanding nature of the service member's environment and conditions. For example, the complete electronics and power train package can easily be removed in the case of a malfunction in a field condition, so that the device transforms into a conventional prosthesis.

Public Purpose: A transtibial prosthetic device that satisfactorily mimics able-bodied gait can be used by the general public. Because of the prevalence of diabetes, the number of below-the- knee amputees will increase greatly. In the first year, we found that the subject's health improved because he was briskly walking on a treadmill with a powered prosthetic device.

Body

The **SPARKy** Project (Spring Ankle with Regenerative Kinetics)

Even today's most sophisticated microprocessor controlled foot-ankle prosthetic devices are passive. They lack internal elements that actively generate power, which is required during the "push-off" phase of normal able-bodied walking gait. Amputees must rely upon the limited spring-back available within the flexed elastic elements of their prostheses to provide power and energy and thus must modify their gait through compensation. Consequently, lower limb amputees expend 20-30% more metabolic power to walk at the same speed as able-bodied individuals. A key challenge in the development of an active foot-ankle prosthetic device is the lack of good power and energy density in current actuator technology. Human gait requires 250W of peak power and 36 Joules of energy per step (80kg subject at 0.8Hz walking rate). Even a highly efficient motor such as the RE75 by Maxon Precision Motors, Inc. rated for 250W continuous power with an appropriate gearbox would weigh 6.6 Kg. This significant weight is only the actuator and transmission. It does not include the electronics or the batteries.

In the first year, we designed the *Spring Ankle with Regenerative Kinetics (SPARKy)* which uses a new generation of powered prosthetic devices based on the Robotic Tendon actuator. This actuator is a lightweight motor and lead screw in series with a helical spring that significantly minimizes the peak power requirement of an electric motor and total system energy. The kinetic advantages of the Robotic Tendon will be shown along with the electro-mechanical design and analysis that will provide SPARKy users with 100% of required push-off power and ankle range of motion comparable to able-bodied ankle motion while maintaining a form factor that is portable to the wearer.

In the second year, we developed and tested a transtibial prosthesis that will support continuous unstructured walking for up to 2.8 hours. A pilot study with 2 subjects tested the device. An independent gait laboratory will compare gait symmetry and metabolic consumption of SPARKy versus the subject's conventional prostheses. All components are worn and are lightweight and portable.

SPARKy Project Overview

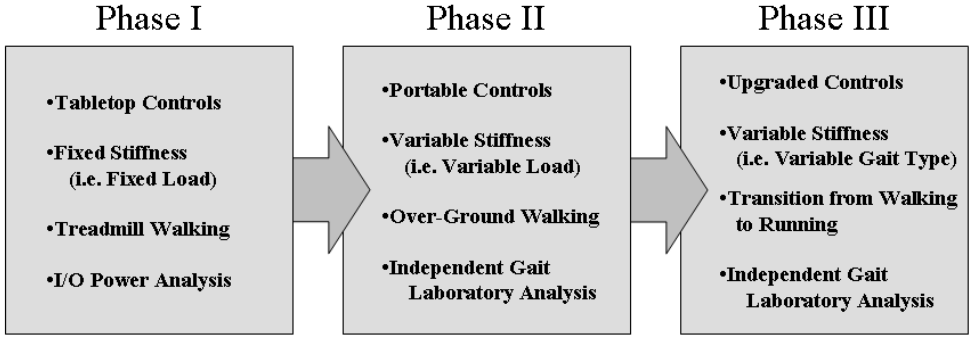

Phase 2. To develop, test and demonstrate a transtibial prosthesis for over ground unstructured walking (Months 13-24):

a. Design and build SPARKy 2a with the capability to support continuous, unstructured walking for up to 2.8 hours. Mechanical tunability and sensor feedback will allow for variations in load, speed, and environment within the bounds of walking. All componentry will be lightweight, self-contained, and portable. (Months 13-20).

SPARKy 2a has been designed and built. Testing of the mechanical design is on going. A microprocessor has been chosen and code has been ported to the microprocessor. The microprocessor unit has been attached to the device and drives a brushed RE40 DC motor.

b. Bounds of walking (up to 2 m/s) will include walking on flat even surfaces, walking on inclines/declines, and ascending/descending stairs

As part of a separate project, able-bodied data has been collected at Brooke Army Medical center for walking, walking on inclines/declines, and ascending/descending stairs. The able bodied data is being analyzed. We are developing continuous based controllers, not state based controllers that can be fooled. Matthew Holgate is studying the relationship between the Tibia elevation angle and the foot elevation angle.

We are able to walk continuously over ground and can walk up and down slopes and stairs. Walking up a slope and ascending stairs needs to be improved, adding extra propulsion. The propulsion walking down stairs needs to be reduced.

c. Test and iterate the design with two selected transtibial amputees at Arizona State University.

A second subject has been recruited and a new socket has been manufactured. The second subject has successfully worn SPARKy 2a.

d. Testing will include motion capture and oxygen consumption measures and will be independently conducted by another research team at Washington University, Saint Louis, MO. (Months 21-23).

SPARKY 1a has been delivered to Washington University on January 11, 2009 for initial fitting and testing. The testing has started and will be completed by September 2009.

e. Demonstrate SPARKy II to Brooke Army Medical Center. (Month 24). Date still must be determined.

2.0 Design, Build, Test and Demonstrate SPARKy 2a	**Months 13-24**	Support continuous unstructured walking for up to 2.8 hours. Mechanical tunability and sensor feedback will allow variation in load, speed, and environment within the bounds of walking, 1 to 2m/s. All componentry will be self-portable	Thomas Sugar, Project leader
2.1 Upgrade Prosthesis Componentry for over ground walking	**Months 13-14**	Support walking with powered element.	PhD student 1: Holgate
2.2 Design, Build and Test prosthesis	**Months 13-16**	1 DOF using SPARKy I control software.	Holgate
2.3 Design, Select/Build, Package and Test Wireless and Portable Electronic Components	**Months 14-17**	Interface with prosthesis. Show functionality using SPARKy I control software.	Robotics group Thierry Flaven
2.4 Assemble Hardware	**Month 17**	IAW Hardware Specs/drawings. Supports limb to limb symmetry.	Thierry Flaven
2.5 Design, Develop and Test Control Scheme	**Months 14-18**	Show logical output signal to motor based on sensor input signals.	Jeffrey Ward Holgate
2.6 Integrate System Hardware, Software and Control	**Months 19-20**	IAW System Specs.	Holgate Thierry Flaven
2.7 System Performance Tests and Iterations	**Months 21-22**	Support continuous unstructured walking for up to 2.8 hours. Mechanical tunability and sensor feedback will allow variation in load, speed, and environment within the bounds of walking, 1 to 2m/s. All componentry will be self-portable (within prosthesis or fanny pack.)	Arise Prosthetics Holgate Thierry Flaven
2.75 Independent Motion Capture and Oxygen Consumption Test	**Month 23**	SPARKy 2a should require 20-30% less metabolic power than amputees supported by commercial foot-ankle devices.	Dr. Jack Engsberg, Motor Analysis Laboratory
2.8 System Demonstration	**Month 24**	Show continuous unstructured walking. Adjust speed (1 to 2 m/s)	Sugar Holgate Thierry Flaven Mark Werner

Deliverables:

1. Design and construction of SPARKy 2a - **Completed**
2. Develop a rate gyro based controller for over ground walking - **Completed**
3. Test able bodied subjects walking on flat even surfaces, inclines/declines, and ascending/descending stairs – **In Process**
4. Using able bodied test data, a controller will be developed for over ground walking that includes inclines/declines and ascending/descending stairs – **In Process**
5. Develop a compact microprocessor - **Completed**
6. Develop a compact brushless DC motor amplifier – **Stopped working on this item**
7. Port Matlab code to microprocessor **Completed**
8. Test SPARKy 2a on two transtibial amputees at Arizona State University Conduct and Independent Motion Capture and Oxygen Consumption Test. **In Process**

Progress for Months 1-12

Activity 2.1 Upgrade Prosthesis Componentry for over ground walking.

We purchased a very lightweight, durable, and robust roller screw. The motor and roller screw have been ordered and received.

The roller screw has worked very well, but the brushless DC motor has not worked well. The need for Hall Effect sensors and high frequency modulation of the voltage has discouraged the use of the ECPowermax 30. We are currently using the RE40 motor.

Activity 2.2 Design, Build and Test prosthesis.

SPARKy 2a has been designed in SolidWorks and all parts have been ordered and assembled.

Figure 1. SPARKy 2a: It will weigh less than 1.8 kg and will use a RE40 DC motor along with a custom roller screw. The sole of the shoe to the top of the Robotic tendon measures 12.9 inches.

- The refined SPARKy design uses the RE40 motor, roller screw robotic tendon and FS3000 keel.
- Total Weight: 5 lbs not including socket
- Box Dimensions: 9.6 L x 3.7 W x 12.9 H (inches)
- Min. Clearance Height: 5.5 inches

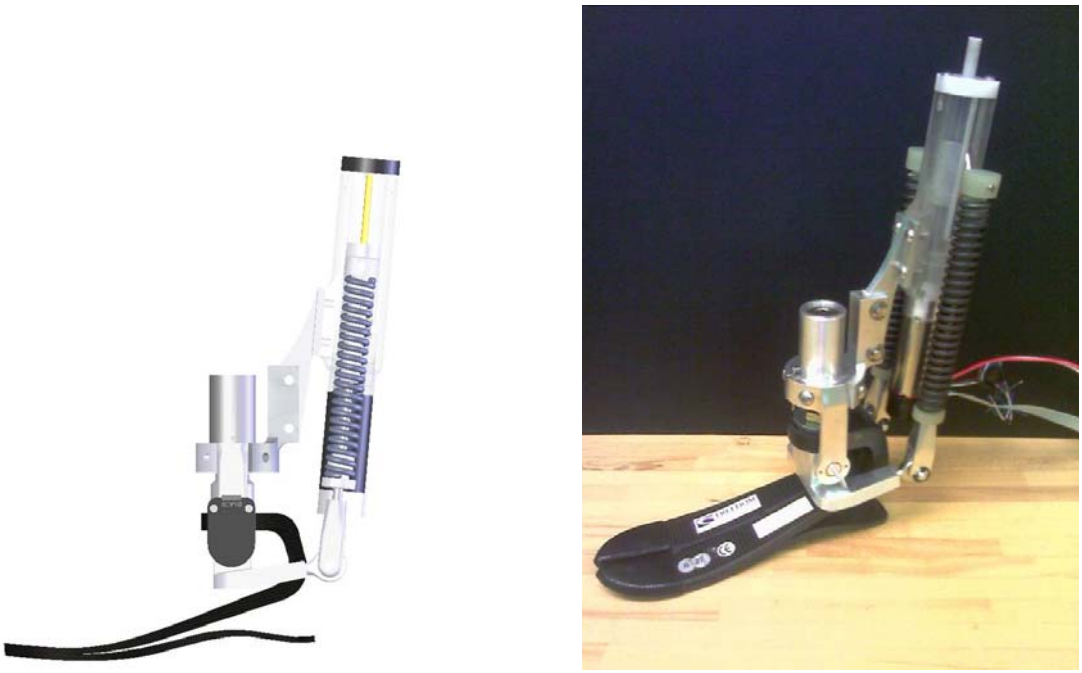

Figure 2. SPARKy 2a: Side View, Assembled robot

Activity 2.3 Design, Select/Build, Package and Test Wireless and Portable Electronic Components

Thierry Flaven has selected the dsPIC 33 microprocessor. We have purchased a Demo board, MPLAB, and the Kerheul Matlab blockset. We have ported the Matlab code over to the dsPIC microprocessor board. We tested the microprocessor by controlling the SPARKy 1a foot. Hand testing was performed and is shown in Figure 3.

Figure 3: In the left picture, the microprocessor demo board is controlling a standard DC motor. In the right picture, Matthew Holgate is using a pole attached to the robotic foot to test the microprocessor controller.

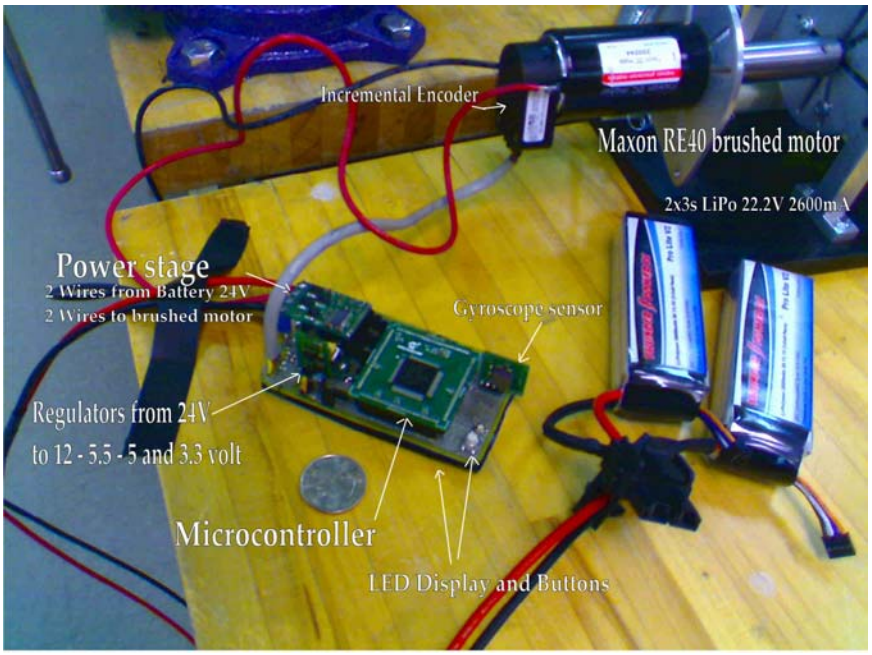

Figure 4: The custom microprocessor board is controlling a Maxon RE40 DC motor.

Activity 2.4. Assemble Hardware

Two tasks were completed to assemble the hardware. In task 1, the new robot, SPARKy 2a, was attached to a table top controller using a commercial brushless DC controller. We tried the following three brushless controllers and only the PMD board worked: (PMD DK 731110, APEX SA306-IHZ, and Maxon DES 70/10). This conservative approach allowed us to test the new robot while walking on the treadmill, walking when the treadmill is inclined, and walking when the treadmill is declined.

In task 2, we designed a standalone dsPIC 33 board that controls a brushed DC motor controller. A small brushless DC motor controller has been very hard to design because we need to add three large inductors to the motor coils. We hoped to use two APEX motor control boards but the power output was too low.

In task 2, we dropped the EC Powermax motor and are using the RE40 motor. We have assembled all of the hardware, see Figure 4.

Activity 2.5. Design, Develop and Test Control Scheme

Matthew Holgate has designed a Tibia Based controller that runs a continuous control algorithm. It can determine gait percent in the first 0.001 seconds of gait initiation. We use the phase angle of the tibia to determine gait percent. The polar length of the phase vector determines stride length. By knowing stride length and gait percent, we can determine the person's desired walking speed. Over ground walking has been demonstrated using this controller.

Matthew Holgate is now analyzing able bodied data when walking on inclines and declines to determine a 2nd Tibia Based controller for these secondary tasks.

Activity 2.6. Integrate System Hardware, Software and Control

We have integrated the electronics, software to the robot.

Activity 2.7. System Performance Tests and Iterations

We have completed performance tests. We are able to walk consistently over ground.

Activity 2.75. Independent Motion Capture and Oxygen Consumption Test

We took SPARKy 1a to Washington University on January 11, 2009 for initial testing and fitting.

Activity 2.8. System Demonstration

Planned for August 2009.

Figure 5: Subject is walking over ground on a flat surface.

Figure 6: Subject is walking on an inclined surface where the angle is constantly changing. Two small batteries are carried at the waist.

Figure 7: Subject is able to ascend and descend stairs.

Shank Based Controller

In the phase 2, we developed a tibia based controller or a "shank based controller." Our goal was to develop a continuous based controller for walking. We wanted to eliminate the need for state based control and heel strike sensors. In our phase 1 research, if the heel strike sensor was not pressed, then the motor pattern was not initiated. Also, the user can be tricked by a state based controller if each state is not initiated in the correct pattern. Lastly, it is tricky to formally test a state based controller because all of the different states must be tested in multiple scenarios. Testing 4 states in 4 scenarios could lead to testing 4 to the power 4 cases which equals 256 trials.

We measured the shank angle in world coordinates for different stride lengths, see Figure 8. Calculating the gait percent uniquely from this curve is not possible. For example, the angle 0 degrees corresponds to approximately 35% and 88% of gait.

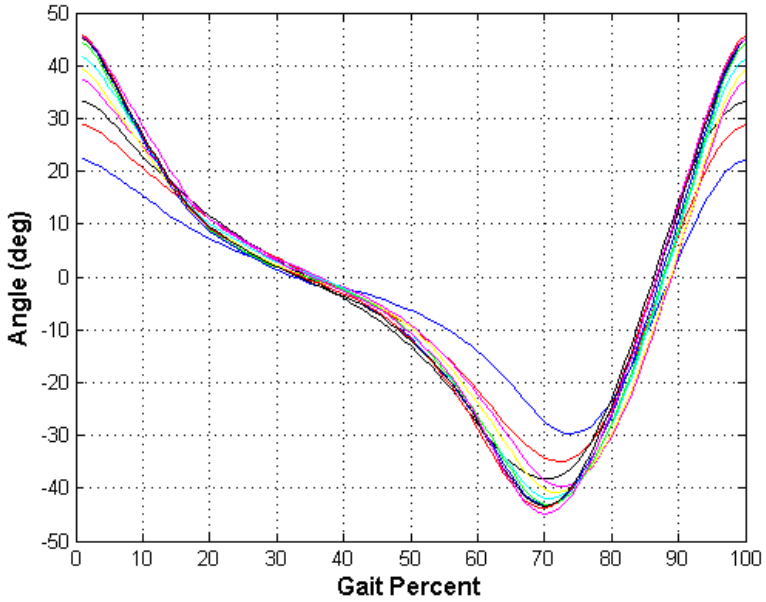

Figure 8: Shank angle in world coordinates for different stride lengths.

We then decided to use phase angles which allowed for a unique one-to-one correspondence between shank phase angle and gait percent. The phase plot is constructed by plotting the shank angle versus shank angular velocity, see Figure 9. In this way, each point in Figure 8 is matched to its corresponding angular velocity. Continuous, oval shaped curves represent a particular gait cycle with a particular stride length. As the stride length is increased, the ovals become larger.

For a particular phase curve, the polar angle, Phi, and the polar radius, r, can be measured. In our analysis, the polar angle starts at 0 degrees, and the radius rotates in a clockwise fashion.

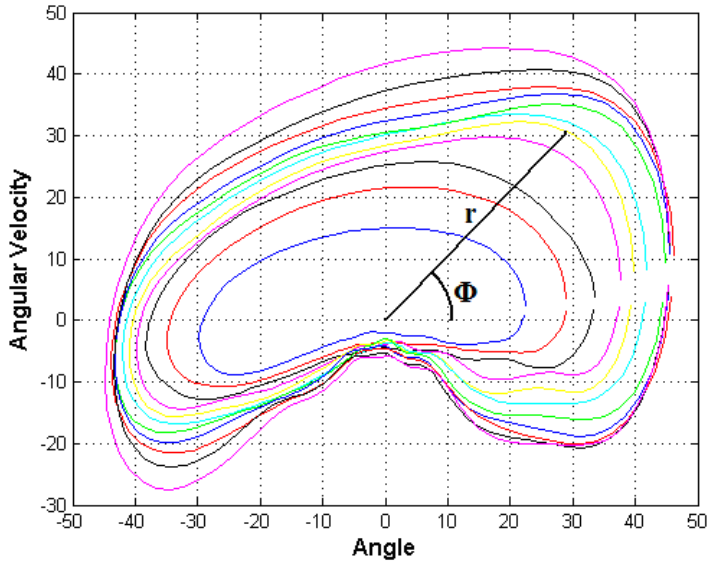

Figure 9: Phase plot of the shank angle versus shank angular velocity. The ovals become larger as the stride length increases. For a particular phase curve, the polar angle, Phi, and the polar radius, r can be measured.

The polar angle is measured as a function of gait percent and is shown in Figure 10. Two important results are shown. Firstly, for each polar angle, there exists one unique gait percent. Thus, if the polar angle is measured in real time on the robot, the gait percent can be calculated. Secondly, the curve of polar angle versus gait percent is invariant to the different stride lengths. We can then measure the polar angle and determine gait percent uniquely regardless of the stride length.

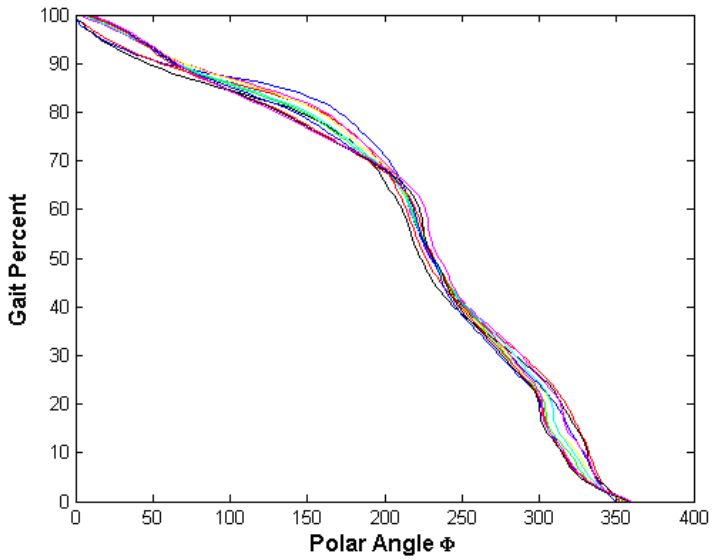

Figure 10: The polar angle is calculated as a function of gait percent. There is one unique polar angle for each gait percent. All of the curves lie on top of each other so that the polar angle is invariant to stride length.

To test our ability at calculating gait percent, a heel strike sensor and a rate gyro were measured while a subject wore the robotic ankle. A straight, diagonal dashed-line was drawn between heel strike sensors to determine a predicted gait percent. The gait percent calculated from the polar angle was drawn using a solid-line. Our method was able to calculate gait percent accurately, see Figure 11.

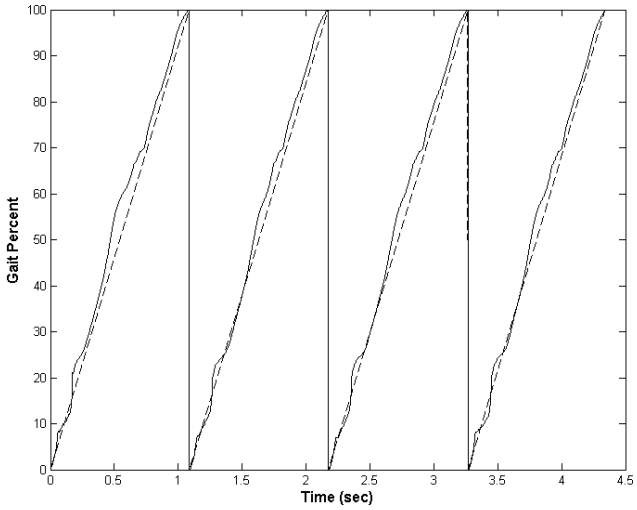

Figure 11: Gait percent is calculated using the polar angle.

The polar radius from Figure 9 is used to calculate the stride length. There was not a one-to-one function between polar radius and stride length. We used a look up table to determine stride length. The polar radius and polar angle are measured and then used to determine the stride length.

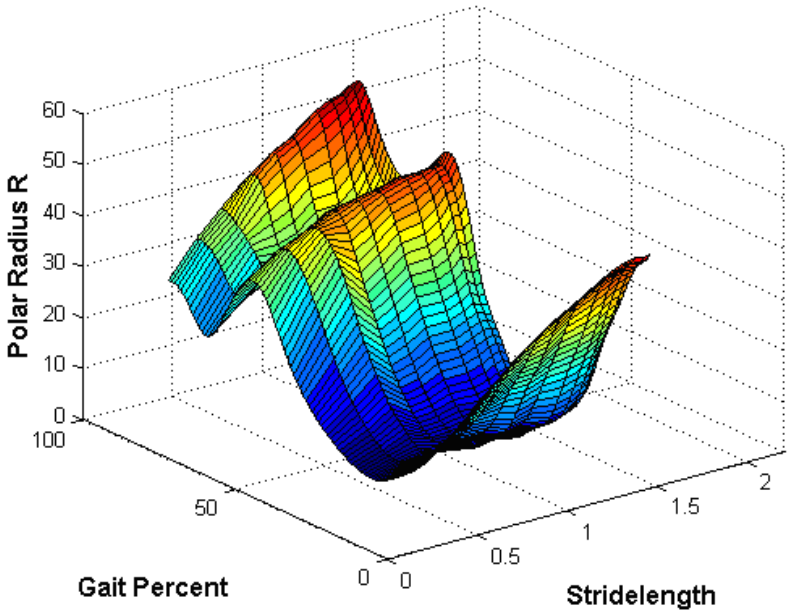

Figure 12: The polar radius and gait percent are used to calculate stride length.

Once the stride length and gait percent are determined, the speed of the user as well as where they are in the gait pattern can be determined. We used these two variables to determine the position of the motor. We used the robotic tendon analysis to determine the deflection of the spring for each gait cycle corresponding to different stride lengths. The deflection of the spring uniquely determines the motor position. We then use a position controller to drive the screw to the correct position.

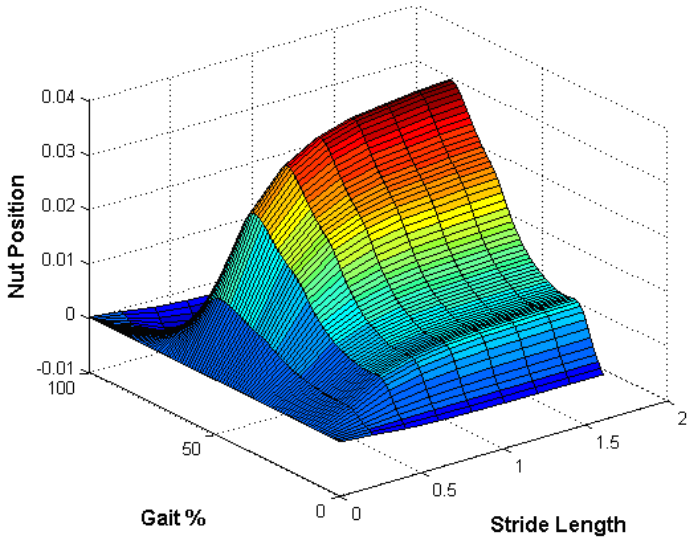

Figure 13: The stride length and gait percent are used to determine the motor position.

In summary, we are developing a continuous based controller based on the phase plot of the tibia angle. The phase angle determines gait percent regardless of stride length. The polar radius is a measure of the stride length. The stride length and gait percent determine the proximal position of the spring in the robotic tendon. We use a simple position controller to adjust the proximal position of the spring.

In our lab, we are now using gait surfaces instead of gait curves.

Key Research Accomplishments:

Our powered ankle devices include the following characteristics:

- User has full range of sagittal ankle motion comparable to able-bodied gait. (23 degrees of plantar-flexion, 7 degrees of dorsiflexion.)
- User has 100% of the required power for gait delivered at the correct time and magnitude.
- The peak output power is 3-4 times larger than the peak motor power allowing a reduction in motor size and weight.
- Provide the user the flexibility to easily remove and install the Robotic Tendon to allow SPARKy to be used as a “powered and computer controlled” prosthesis or a “standard” keel and pylon prosthesis
- Based on lightweight, energy storing springs
- Allows a highly active amputee to regain high functionality and gait symmetry
- A demonstration of a powered, transtibial prosthesis was performed on November 2nd, 2007 at The Center for the Intrepid, Brooke Army Medical Center.

Phase 2:

- Roller screw transmission was very robust and lightweight.
- A compact microprocessor was developed.
- Over ground walking was demonstrated.
- Walking on inclines and declines was demonstrated.
- Ascending and descending stairs was demonstrated.

SPARKy’s biggest advantage lies in the fact that we are storing energy in a spring uniquely chosen for an individual. If one chooses the correct stiffness, the spring can be adjusted by the motor to allow for a 3 to 4 times power amplification. Because we have a large power amplification, we can use a small motor allowing a very large sized user to walk slow or walk at a very fast pace. Currently, we are only using 55 Watts of a 150 Watt motor so that we can easily power large individuals and can power fast walking.

We are using a fully intact keel that will absorb the heel strike impact and allow for correct rocker motion over the heel. The Robotic Tendon can be detached so that it can

be easily removed reverting back to a standard, passive carbon fiber keel. This feature can provide an alternative if the electronics fail in a field condition.

We are focused on developing the most durable, versatile, and powerful walk/run prosthetic ankle that meets the goals of a highly functional Military amputee. Because of our power amplification, we can easily walk very fast and have confidence in building a walk/run device for Year 3.

Reportable Outcomes

- Manuscripts
    - one PhD dissertation,
    - one MS thesis
    - four conference papers were published
    - one journal paper was submitted
    - one journal paper was published

- Popular Press – multiple web pages and newspaper articles discussed research

- Presentations – presented research at Dynamic Walking 2008 and 2009

- Demonstrations – Brooke Army Medical Center, Center for the Intrepid, November 2007

- Joseph Hitt earned his PhD in May 2008

- Ryan Bellman earned his MS in August 2008

Conclusion

Significant advances have been achieved towards creating a computer-controlled, powered transtibial prosthesis that can actively support a user in their normal environment and conditions. Low power, high energy consumption, and sophisticated control methodology are key challenges towards realizing a smart, powered prosthesis. In Phase 1, the SPARKy project was able to develop a prosthesis that could supply high peak power to the user at push off in a light weight and energy efficient device.

The key outcomes included:

1. the user has full range of sagittal ankle motion comparable to able-bodied gait. (23 degrees of plantar-flexion, 7 degrees of dorsiflexion, and
2. the user has 100% of the required power for gait delivered at the correct time and magnitude.

The device provides the user 100% of the ankle power and ankle joint movement similar to able-bodied gait. This unique device is one of the most powerful and efficient devices of its kind.

The analyses and test data show that the motor power can be amplified to provide the user 100% of the required power. We showed a power amplification of the output power compared to the input power of 3 to 4 times. This power amplification allows the downsizing of the actuator to a portable level. For example, a small 150 W motor in combination with a transmission and spring provides 200 W to 400 W during testing. This size and weight of the system is to a level that is comfortably portable to the user while powerful enough to support an 80 kg subject up to his maximum walking speed of 1.8 m/s (4 mph). The data suggests that there is enough power available to support even larger users at such speeds.

In Phase 2, the SPARKy project developed a very lightweight prosthesis that was used in over ground walking. The roller screw design was very successful because it was a very robust and lightweight transmission. We ported all of the code to a dsPIC 33 microprocessor. Finally, this project exceeded our expectations in terms of the device performance. Our new control methodology and embedded microprocessor control allowed our Phase 2 device to move from the laboratory to the unstructured and highly dynamic environments that include stairs, inclines/declines and over ground walking.

These demands are very challenging but our successful Phase 1 and 2 research efforts provide the team high confidence that a walk/run device is possible.

References

Popular Press:

1. Next generation of powered prosthetic devices based on lightweight energy storing springs. What's next network - Science and Technology - May 2, 2007

2. "Sparky;" the Ankle Prosthetic of the Future, Med Gadget - May 2, 2007

3. Researchers create next generation prosthetic devices - News-Medical.net - May 2, 2007

4. ASU researchers putting new spring into amputees' step, MSN Money, May 1, 2007

5. Smart Prosthesis of the future created, United Press International - May 3, 2007

6. Smart Prosthesis of the future created, Podiatry News , Foot News - May 3, 2007

7. The World's First Powered Ankle, Technology Review - By Emily Singer and Duncan Graham-Rowe - May 11, 2007

8. SPARKy the prosthetic ankle set to "revolutionize prosthetics"
Posted May 3rd 2007 by Paul Miller

9. ASU, Walter Reed researchers create prosthesis of the future, ASU Insight -May 11, 2007

10. Innovations Report -By Chris Lambrakis - May 03, 2007
EurekAlert - May 1, 2007
Brightsurf Science News - May 2, 2007
FusePress - May 2, 2007
Medical News Today - May 3, 2007
newsrx.com - May 1, 2007
ScienceDaily - May 2, 2007
VA News Flash - VA Watchdog dot Org By Larry Scott at -May 03, 2007
First Science News - May 1, 2007

11. Discovery News - By Tracy Staedter - May 31, 2007

12. Arizona researchers putting new spring into amputees' step
The Business Journal of Phoenix - May 1, 2007

13. Washington Business Journal -by Ty Young May 3, 2007
Researchers take step forward in design of new prosthesis

14. Discovery Channel, 2008, "Toad research could leapfrog to new muscle model", show was called "Toady Tendons", December 3, 2008, 8 minutes

15. National Geographic, January 2010, Applied Bionics

Conference Papers:

M. Holgate, J. K. Hitt, R. D. Bellman, T. G. Sugar, K. W. Hollander, "The SPARKy (Spring Ankle with Regenerative Kinetics) Project: Choosing a DC Motor Based Actuation Method," Biorobotics 2008.

R D. Bellman, T. G. Sugar, "SPARKy 3: Design of an Active Robotic Ankle Prosthesis with Two Actuated Degrees of Freedom Using Regenerative Kinetics," Biorobotics 2008.

M. A. Holgate, A. W. Boehler, T. G. Sugar, "Control Algorithms for Ankle Robots: A Reflection on the State-of-the-Art and Presentation of Two Novel Algorithms," Biorobotics 2008.

J. Hitt, R. Bellman, M. Holgate, T. Sugar, and K. Hollander, The SPARKy (Spring Ankle with Regenerative Kinetics) Project: Design and Analysis of a Robotic Transtibial Prosthesis with Regenerative Kinetics, ASME International Design Engineering Technical Conference, CD-ROM, pp. 1-10, 2007.

Journal Papers:

Hitt, J, Holgate, M, Bellman, R, Sugar, TG, Hollander, KW, Accepted, "Robotic Transtibial Prosthesis with Biomechanical Energy Regeneration", Industrial Robot: An International Journal, 2009.

Joseph K. Hitt, Matthew Holgate, Thomas G. Sugar, Ryan Bellman and Kevin W. Hollander, "Building an Energy Efficient Robotic Transtibial Prosthesis: The SPARKy (Spring Ankle with Regenerative Kinetics) Project, *submitted* to ASME Journal of Mechanisms and Robotics.

Dissertation:

Dissertation: A Robotic Transtibial Prosthesis with Regenerative Kinetics, Joseph Hitt, Arizona State University, May 2008.

Thesis:

Thesis: Mechanical and Conceptual Design of a Robotic Transtibial Prosthesis, Ryan Bellman, Arizona State University, August 2008.

Appendices

Three conference papers and a journal paper are attached.

Journal:
1. Hitt, J, Holgate, M, Bellman, R, Sugar, TG, Hollander, KW, Accepted, “Robotic Transtibial Prosthesis with Biomechanical Energy Regeneration”, Industrial Robot: An International Journal, 2009.

Conference:

1. M. Holgate, J. K. Hitt, R. D. Bellman, T. G. Sugar, K. W. Hollander, “The SPARKy (Spring Ankle with Regenerative Kinetics) Project: Choosing a DC Motor Based Actuation Method,” Biorobotics 2008.

2. R D. Bellman, T. G. Sugar, “SPARKy 3: Design of an Active Robotic Ankle Prosthesis with Two Actuated Degrees of Freedom Using Regenerative Kinetics,” Biorobotics 2008.

3. M. A. Holgate, A. W. Boehler, T. G. Sugar, “Control Algorithms for Ankle Robots: A Reflection on the State-of-the-Art and Presentation of Two Novel Algorithms,” Biorobotics 2008.

Control Algorithms for Ankle Robots: A Reflection on the State-of-the-Art and Presentation of Two Novel Algorithms

Matthew A. Holgate, Alexander W. Böhler, Thomas G. Sugar

***Abstract*— With computer speeds greatly increasing, hardware is no longer a hurdle in the development of controllers for wearable lower limb robots. The challenge remains in developing smart algorithms that are able to detect which task a person is about to perform and then supply the robot with the correct desired movements. This paper reflects on some existing control algorithms and then presents theory and test results of two novel concepts. The goal of this paper is to show that the two new concepts are capable of producing the correct motor profile.**

I. Introduction

Many people could benefit from a powered ankle. There are approximately 1.35 million people in the U.S. who are living with an amputation of the lower limbs and it is estimated that this number will more than double by the year 2050 [1], [2]. Moreover, there are about 4.7 million stroke survivors alive today in the United States, with about 700,000 more cases each year [3]. Many of these stroke survivors could use a powered ankle foot orthosis. These numbers do not include other groups of people such as the elderly or people who suffered from a different neurological injury, who could also benefit from a powered ankle.

When building these robots, the challenge now is to develop sophisticated controllers since the mechanical systems in many cases have already been refined [4], [5], [6], [7]. In controls, it is no longer the hardware that is a bottleneck, but determining the user's intention is a very difficult challenge. One must determine smart and sophisticated algorithms that are able to sense which task a person is about to perform and then generate the the correct robotic movements. There are numerous tasks that a person performs during every day life, ranging from normal walking, to climbing stairs, walking up or down a slope, or even just balancing their legs while they are standing and talking to another person.

This paper firstly will reflect on some of our existing control methods and then present the theory and test results for two novel control concepts for wearable ankle robots.

II. Existing Control Algorithms

Over the past couple of years, several different control algorithms have been developed to control wearable robots for the lower limbs. In this section some of the existing controllers are shown and briefly analyzed. The control algorithms presented in the first three sections have a structure shown in Fig. 1, where a DC motor is controlled in series with a transmission and linear spring that is attached to the ankle.

A. Basic Nut Control

One possibility to control a robot with the structure in Fig. 1 is to control the position y (which in this case is the position of the nut on the lead screw), which is the backside of the spring. The actual nut position y_a can easily be measured with a motor encoder and then subtracted from a given reference command r.

However, limitations are reached with a fixed nut pattern as soon as optimization of the controller for certain stages during gait is desired, or if one wants the reference command, which essentially is a gait pattern, to adjust itself for different walking speeds or different activities such as walking versus stair climbing. Oymagil et al. [8] have shown the adjustment of a pattern *only* in its duration in time; however, there are limitations since the amount of plantarflexion varies with speed as well. For example, when walking slowly, the behavior of the robot feels unnatural. A dynamic pace controller is described in this paper to adjust the nut pattern both in time and in shape.

B. Robust Control

In [9] the authors describe an algorithm, which combines velocity and stiffness control. The stance phase of gait is split into five different zones and each zone is governed by velocity or stiffness control as shown in Fig. 2. For *zone 1*, which starts at heel strike, the author suggests to use velocity control to keep the motor velocity constant and at a level proportional to the speed of the previous swing phase.

Zone 2 starts when the ankle angular velocity, $\dot{\theta}$, crosses through zero. For this zone it is suggested to maintain a constant stiffness which is 1.35 times the actual spring stiffness.

For, *zone 3*, which starts at flat foot and occupies most of the loading phase, again a constant stiffness should be applied which is 3 times the actual stiffness of the spring.

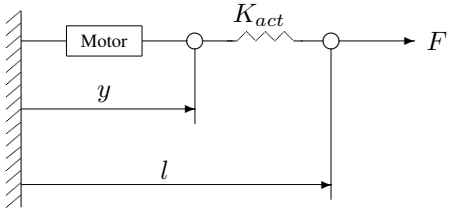

Fig. 1. Model for an actuator for the lower limbs

Manuscript received April 23, 2008.

Matthew A. Holgate is with Arizona State University, Tempe Campus, matthew.holgate@asu.edu

Alexander W. Böhler is with Arizona State University, Tempe, Arizona 85287-6106 alexander.boehler@asu.edu

Thomas G. Sugar is with Arizona State University, Polytechnic Campus, thomas.sugar@asu.edu

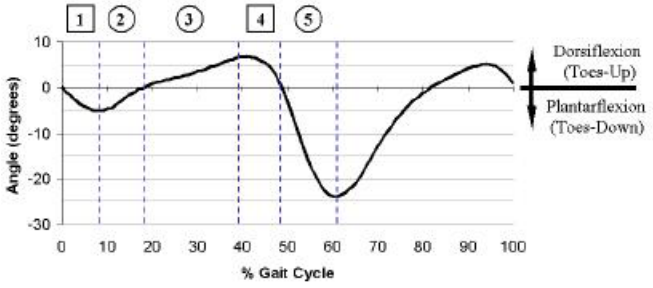

Fig. 2. The stance phase of gait split into 5 distinct zones.

Zone 4 starts when the heel lifts off the ground. It is suggested to maintain a constant velocity during this zone that is equal to the motor velocity in the previous zone.

Zone 5 starts as the body can no longer resist the energy that was stored in the spring and therefore the energy is released which propels the body forward. For this phase it is important for the motor to just "hold position", hence allowing the energy to be released. The end of this zone is when all the stored energy of the spring has been released and the swing phase begins.

Good first test results have been achieved with this method and this algorithm is currently being optimized and tested in more detail. What is really promising about this approach is that the shape of the motor profile is determined by only a few (five) numbers. These are the velocities and stiffnesses that need to be set for each zone. By "tuning" with these numbers, curves with different shapes can be produced, hence, our hope is that we can use this basic controller structure to produce profiles for different activities, such as climbing stairs or walking on different types of ground, simply by changing these parameters in an appropriate way.

C. Impedance Control

In this rather extensive control method a mass-damper-spring relationship between a position x and force f is established as shown in (1).

$$f = m_d\ddot{x} + b_d\dot{x} + K_d x \tag{1}$$

Herein m_d, b_d and K_d denote desired or virtual inertia, damping and stiffness of the system. The advantage of this control method is its flexibility. It allows one to change the effective dynamics of the robot, hence, the resistance of the robot to variations in its environment, such as different types of ground. This requires, however, that one knows the force f that the robot experiences with its environment [10].

Blaya and Herr have shown that impedance control can assist patients with drop-foot gait. Two drop-foot patients were tested with their AAFO with zero, constant and variable impedance control strategies. They found that constant impedance control eliminated the occurrence of foot slap at slow and self-selected speeds. Furthermore, their variable impedance control strategy was able to increase the amount of swing dorsiflexion which helps with toe drag, a second major complication that drop-foot patients experience [11].

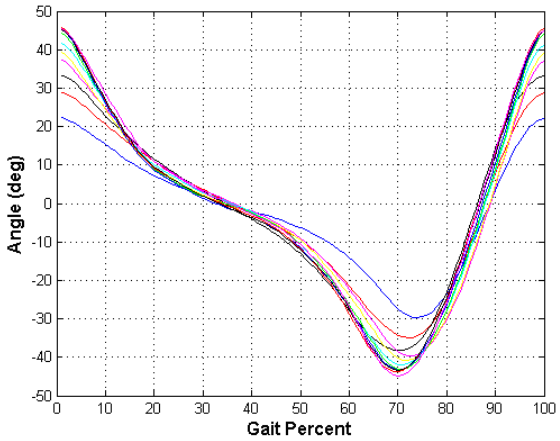

Fig. 3. Tibia angle profile for able bodied human gait. Each curve represents a different stride length. The closer the curve is to the zero degree axis, the shorter the stride length.

D. Myoelectric Control

As mentioned before, one of the main challenges with controlling artificial limbs is to detect which activity the person is about to perform. All algorithms presented to this point measure positions, forces, states, etc. and then try to find a unique shape in these curves that enables the algorithm to make a decision. Hence, the question arises, why not measure the EMG signals. EMG signals are measured by electrodes, filtered and used as reference commands.

Ferris et al. [12], [13] have used EMG signals from the soleus and tibialis anterior to control their pneumatically powered AFO. The raw EMG signals were firstly passed through a second order high-pass filter to remove movement artifacts. Then the signals were full-wave rectified and passed through a second order low-pass filter to obtain a smooth control signal. A threshold is used to eliminate background noise and the signal is scaled by an adjustable gain to calculate the final control signal.

Test results with their improved powered AFO showed that the person was able to walk immediately after turning on the proportional myoelectric control. The pneumatic muscles supplied 36% plantar flexor torque and 123% dorsi flexor torque.

Challenges that remain with this controls approach are the process of obtaining a robust control signal from the raw EMG signals and that there are many factors that influence the correlation between surface electromyography amplitude and biological muscle force.

III. Novel Controllers

A. Tibia Based Controller Theory

The tibia based controller seeks to find a measurable variable to determine a mathematical relationship between the tibia angle and ankle angle. The tibia global angular position (world based coordinates) was chosen for this relationship because of its simple shape (Fig. 3). Looking at the different curves shown in Fig. 3, it is important to notice that each different stride length produces an almost identical curve, only scaled by some function of stride length. It is also

of note that if the curve is divided into two parts at the minimum around 70% gait cycle, each resulting half becomes an invertible function of gait percent. Each half can also be distinguished from one another by the slope of each curve, which is negative for the first half and positive for the second half. Measurement of the tibia angle can also be accomplished with a sensor attached to the prosthetic device and requires no additional measurements or sensors on other body parts. The aforementioned characteristics make the tibia global angle a wise choice for a prosthetic controller.

Since previous controllers have shown that using logic to make gait decisions can create situations in which the controller is fooled, it is desired that the tibia based controller be completely continuous. To accomplish this, a relationship between the tibia angle and desired ankle angle is required. As previously mentioned, the tibia angle versus gait percent curve (Fig. 3) is not invertible as a whole. To make a function that is solvable, the tibia angular velocity dimension is added and the curve is plotted with tibia angle on the horizontal axis and tibia angular velocity multiplied by a scaling factor on the vertical axis. The resulting curves shown in Fig. 4, are for increasing stride length as the curves get larger. The coordinates in Fig. 4, instead of being represented in Cartesian coordinates of angle and angular velocity, will be represented by polar coordinates Φ and r.

Looking at Fig. 4, it is apparent that the polar angle Φ must be related to gait percent by some function for each different stride length curve. The relationship between Φ and gait percent is plotted for each different stride length in Fig. 5. Of note is the fact that for each different stride length curve, the function relating Φ to gait percent is very close, and is invertible. Also shown in Fig. 5 is gait percent plotted versus polar angle Φ. A fit to this function means that for any stride length, if tibia global angle and angular velocity are measured and the polar angle calculated, the result can be used as an input to the fitted function, giving an explicit relationship between tibia angle and gait percent.

Calculating gait percent is a straightforward operation, but

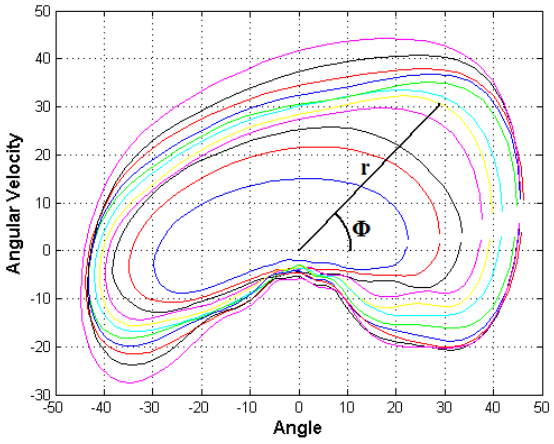

Fig. 4. Tibia angular velocity multiplied by a scaling factor versus tibia angle. The closer the curve is to the origin, the shorter the stride length. Polar angle Φ represents the progression around the curve based on gait percent. r is the polar radius and is related to the stride length of the particular curve.

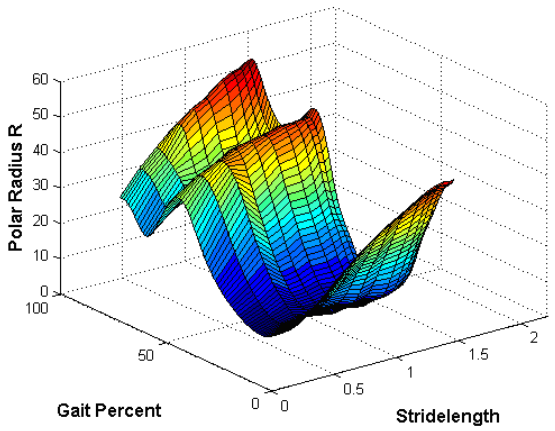

Fig. 6. Polar radius r versus gait percent and stride length. Unlike Φ, r is different for different stride lengths. Note that around 25% of gait cycle the surface is flat along stride length. This creates problems when trying to invert this surface to obtain stride length as a function of gait percent and polar radius.

ankle angles also depend on stride length. Looking back at Fig. 4 it can be seen that in general, the longer the stride length, the longer the polar radius r. However, it must also be noted that any function that relates stride length to r must also be a function of polar angle Φ. The result of plotting polar radius r versus stride length and gait percent is shown in Fig. 6.

It is easy to find how radius r is related to stride length and gait percent; however, the needed relationship is stride length as a function of gait percent and radius r, the two known variables. Looking at Fig. 6 it is obvious that this will be a problem around 25% of gait because the resulting surface will be near vertical and will have multiple values for a single point (gait percent, radius). The reason for this is shown in Fig. 3 at around 25% of gait and Fig. 4 at the bottom middle of the curves where they are bunched up together.

Looking again at Fig. 4 around the problem area at about angular velocity -5 and angle 0, it can be seen that each curve enters the bunched area with a different approach. If a simple first order filter is used on radius r, the curves can be separated. Fig. 7 shows the result of such an approach. The resulting surface is flattened out and for every combination of radius and gait percent there is one value of stride length. It must also be understood that when using an aggressive first order filter, there will be some attenuation and phase lag. This is taken care of by comparing the measured and filtered r not to the actual radius surface (shown as before filter in Fig. 7), but to the expected filtered surface (shown as after filter in Fig. 7).

By implementing the previously discussed method of calculating gait percent and stride length, generating an ankle angle is a simple matter. The ankle angle as a function of stride length and gait percent can be easily measured. The resulting surface can then be fit with a function or a look up table. Depending on what robot is being controlled, the controller will generate a desired position, an example of which is shown in Fig. 8.

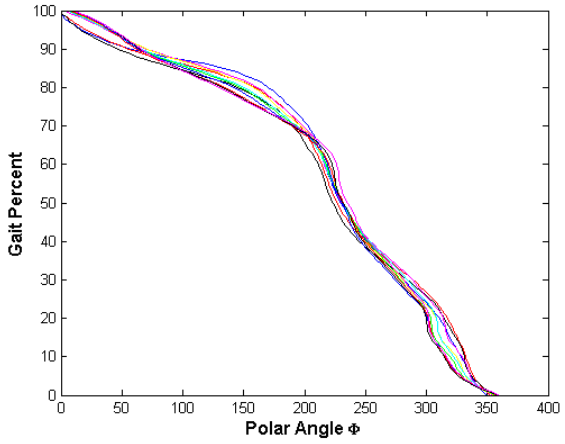

(a) Gait percent of each curve versus the polar angle Φ

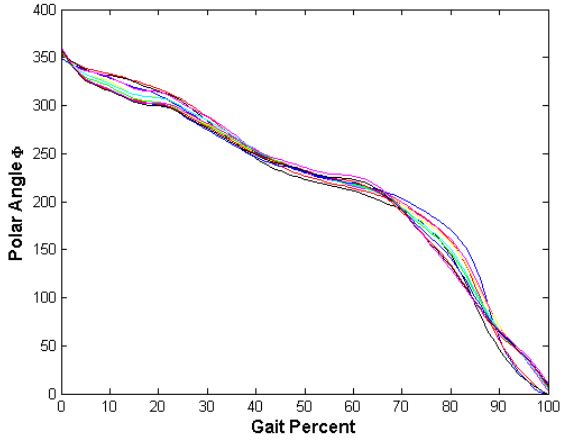

(b) Inverted curves, polar angle Φ versus gait percent

Fig. 5. Note the close relation between all of the curves. The relation between polar angle and gait percent is very close for all stride lengths.

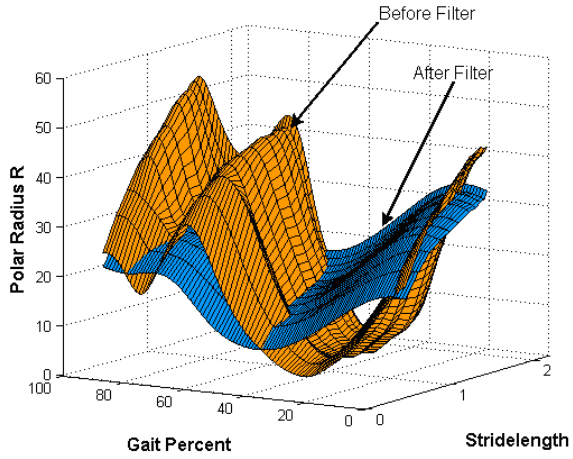

Fig. 7. Same plot shown in Fig. 6 (orange). The blue surface is the result of filtering the polar radius with a first order filter. Note how the new surface can be easily changed to be stride length as a function of gait percent and polar radius.

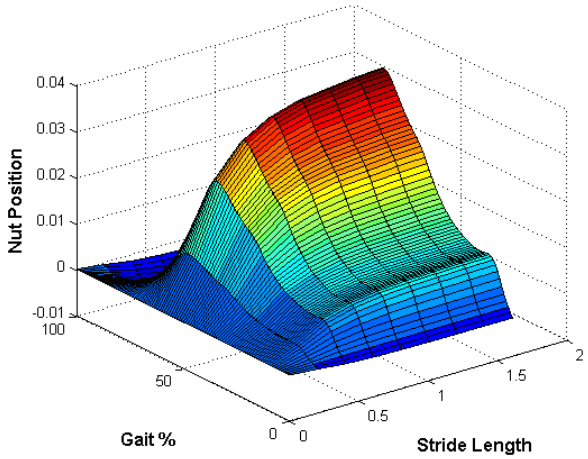

Fig. 8. Position of the nut in meters as a function of stride length and gait percent. Once gait percent and stride length are known, it is simply a matter of looking up the corresponding nut position.

B. Dynamic Pace Control

A second controller being developed in our lab will be discussed next.

Generally, it can be said that the amplitudes of plantarflexion and dorsiflexion become smaller with lower speeds and grow with larger speeds respectively. The latest approach concerning this problem is to adjust the nut profile not only in its duration in time but also in its amplitude.

For the dynamic pace controller firstly a standard motor curve for a stride time of 1 s is calculated. The amount of plantarflexion that this curve provides is then scaled up and down for faster and slower walking. This yields five different nut profiles for five different stride times. To obtain a continuous spectrum of nut profiles depending on the stride time the Fourier coefficients of each profile are calculated using a Fast Fourier Transform (FFT) as shown below, note that the symbols in boldface are matrices. **R** is a 5xn matrix of points describing the five different nut profiles as a percentage of gait.

$$\mathbf{F}_\omega = \text{fft}\,(\mathbf{R}) \tag{2}$$

These coefficients are then fit with a 2^{nd} order polynomial of the form

$$\mathbf{F}_\omega = \mathbf{AT} \tag{3}$$

with the matrices **A** being the coefficient matrix and **T** being the independent variable matrix based on the time duration of each gait cycle. Since **T** is not square we need to multiply (3) with the transpose of **T** first before we can take the inverse and multiply from the right to obtain **A**.

$$\mathbf{A} = \mathbf{F}_\omega \mathbf{T}^T \cdot \left(\mathbf{T}\mathbf{T}^T\right)^{-1} \tag{4}$$

Now, given the matrix **A** and a desired stride time t_s, equation (3) can be used to calculate the Fourier coefficient vector f_ω for the desired stride time. Note that the matrix **T** will become a vector because we are only looking at one

distinct stride time. Taking the inverse Fourier transform then yields the function for the motor reference command.

$$r(t) = \text{ifft}\,(f_\omega) \tag{5}$$

Fig. 9 shows the polynomial fit for the Fourier coefficients and Fig. 10 shows a 3D plot of nut profiles for different stride times, generated with the presented algorithm. It can be seen that time and amplitude of the profiles is adjusted.

Note that the generated nut profiles are also fit with a spline interpolation. This yields a smooth, high quality reference command, which is easy to follow and reduces the overall noise of the motor. As will be seen in IV very good results have been obtained with this method in terms of wearer comfort and power output to input ratios. However, there a few difficulties that remain.

Firstly, one still needs to compute different nut profiles for persons with different weights. Secondly, the controller cannot be optimized for different stages during gait or for different situations. One can easily imagine that, as soon as a person is walking over uneven ground instead of on a treadmill, the whole profile will change as well. Thirdly, this method will always be one gait cycle too late, since it uses the stride time of the last gait cycle to adjust the current gait cycle. These difficulties will be addressed in our future work.

IV. Test Results

A. Tibia Based Controller Implementation and Results

An interesting problem associated with the implementation of such a controller is accurately measuring the tibia global angle and angular velocity. To accomplish this, an angular rate sensor was used. This sensor outputs a voltage proportional to the rate at which it turns. To determine an angle from an angular velocity sensor, it is necessary to integrate the output. However, since the sampling is discrete; the sensor outputs noise; and the integration is numerical, the angle will drift. If the angle drifts away from its true value, the reference ankle angle generated will be completely wrong.

To correct this problem methods such as strap down integration were considered, but were not employed due to the necessity of additional sensors and physical system

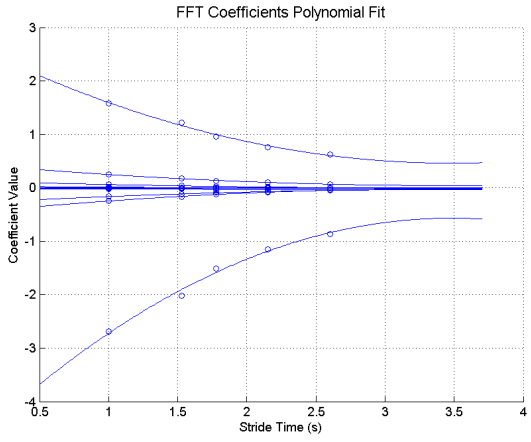

Fig. 9. Polynomial fit for the Fourier coefficients

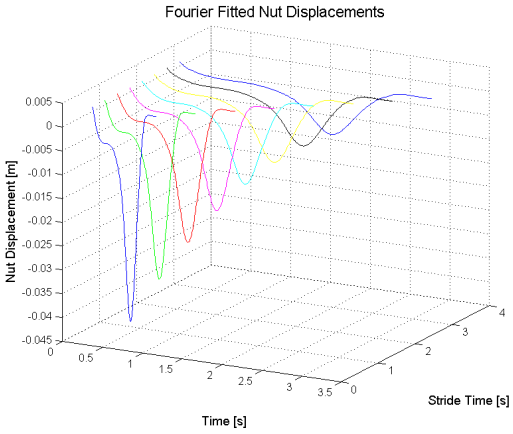

Fig. 10. Nut profiles for nine different stride times

complexity. A digital filter was used to integrate the signal but pulls the resulting signal towards zero. The result is a curve similar to the actual tibia global angle in shape Fig. 3, but centered on the horizontal axis.

It was thought at first that this was not a desirable method because it does not give the true tibia global angle. But in reality, it does not matter what the input is to the controller calculations, as long as the calculations are expecting this input. An added benefit to the filtering method is that it makes actual tibia global angle curves which are slightly different between multiple subjects almost indistinguishable. The result is that the controller can be configured for one person and it will work for almost any user. (Filtered data was calculated when four people walked on a treadmill and over ground.)

For testing the controller, the functions and fits were conducted using data from an able bodied subject. The controller was implemented on the SPARKy robot. An amputee subject walked with stride lengths ranging from very slow to as fast as the subject could walk. The gait percent detection of the controller was always within 5 percent, a very encouraging result shown in Fig. 11. The stride length calculated oscillated smoothly with an error of about 10%. The overall result is a controller that operates smoothly for any stride length or gait percent.

Advantages of the controller include the ability to update the ankle position as fast as the sampling time of the sensors. The controller is never committed to one state of operation looking for another event to decide what to do. For example, the user can take a slow step and in the middle of push off quickly accelerate to a fast walk and the controller will accelerate the ankle. The tibia based controller can also be configured on able bodied persons and operate well on a wide range of users. Another advantage, the details of which are not discussed here, is the ability of this controller to work while walking backwards. In initial tests, the subject was able to take backwards steps using SPARKy while the controller gave a correct ankle motion.

B. Dynamic Pace Test Results

The dynamic pace controller presented in section III-B has been tested several times using an AFO on able bodied

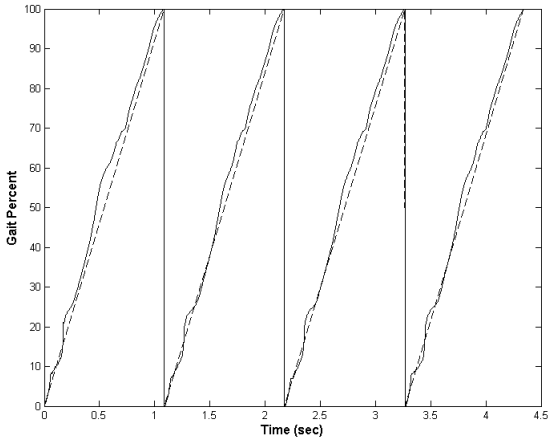

Fig. 11. Gait percent results walking at 2.5 mph. Dotted line is the target value and solid line is gait percent as calculated by the tibia controller.

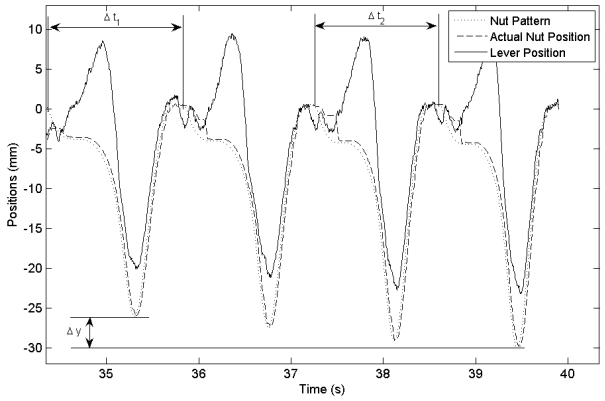

Fig. 12. Kinematics for four consecutive gait cycles

subjects and is currently being tested on stroke survivors. The following results have been obtained from tests on a treadmill with a 70 kg able bodied subject. The first plot in Fig. 12 shows the kinematic curves for four consecutive gait cycles. It can be seen that the amplitudes are adjusted (note Δy) and that the time between two heel strikes is adjusted as well, i.e. note that Δt_1 is greater than Δt_2.

V. Conclusion

This paper has presented existing controllers for prosthetic and orthotic foot-ankle devices. The tibia based and dynamic pace controllers are introduced. It has been shown that both controllers can calculate the necessary reference command. Already in earlier papers [4], [5] our lab has shown that this reference command achieves the requirements for human gait. The tibia controller has the advantage of not relying on any kind of logic to switch between states while only requiring one sensor. This type of controller is much more stable and adaptive to the user. The dynamic pace controller has the ability to change the duration and amplitude of the gait curve simultaneously. A combination of the two controllers is functionally superior to existing controllers.

VI. Acknowledgments

The authors would like to acknowledge the grant that was awarded and administered by the U.S. Army Medical Research & Material Command (USAMRMC), under Contract Number: W81XWH-0710193. The views, opinions, findings, information and presentations made do not necessarily reflect the position of the government and no official endorsement should be made.

References

[1] Ziegler-Graham, K., MacKenzie, E.J., Ephraim, P.L., Travison, T.G., Brookmeyer, R. "Estimating the prevalence of limb loss in the United States: 2005 to 2050". *Archives of Physical Medicine and Rehabilitation 89 (2008)*, pp. 422-429.

[2] Amputee Coalition (2008). [Online]. Available: http://www.amputee-coalition.org

[3] Stroke Center (2008). [Online]. Available: http://www.strokecenter.org

[4] Hitt, J.K., Oymagil, M.A., Sugar, T.G., Hollander, K.W., Boehler, A.W., and Fleeger, J. "Dynamically Controlled Ankle Foot Orthosis (DCO) With Regenerative Kinetics: Incrementally Attaining User Portability", *2007 IEEE Conference on Robotics and Automation (ICRA)*, pp. 1541-1546.

[5] Hitt, J., Bellman, R., Holgate, M., Sugar, T., and Hollander, K., "The SPARKy (Spring Ankle with Regenerative Kinetics) Project: Design and Analysis of a Robotic Transtibial Prosthesis with Regenerative Kinetics", ASME International Design Engineering Technical Conference, CD-ROM, pp. 1-10, 2007.

[6] Dollar, A. M. and Herr, H. "Active Orthoses for the Lower-Limbs: Challenges and State of the Art", *2007 IEEE* 10^{th} *International Conference on Rehabilitation Robotics (ICORR)*, pp. 968-977.

[7] Au, S. K., Weber. J., and Herr, H., "Biomechanical design of a powered ankle-foot prosthesis," Proc. IEEE Int. Conf. On Rehabilitation Robotics, Noordwijk, The Netherlands, pp. 298-303, June 2007.

[8] Oymagil, M.A., Hitt, J.K., and Sugar, T.G., "Control of a Regenerative Braking Powered Ankle Foot Orthosis", *2007 IEEE* 10^{th} *International Conference on Rehabilitation Robotics (ICORR)*, pp. 28-34.

[9] Böhler, A. W., Hollander, K. W., Sugar, T.G., Shin, D. "Design, Implementation and Test Results of a Robust Control Concept for a Powered Ankle-Foot-Orthosis (AFO)". *2008 IEEE International Conference on Robotics and Automation (ICRA)*.

[10] Schaeffer, A.A., and Hirzinger, G., "Cartesian Impedance Control Techniques for Torque Controlled Light-Weight Robots", *Proceedings of the 2002 IEEE International Conference on Robotics and Automation (ICRA)*, pp. 657-663, 2002.

[11] Blaya, J.A., Herr, H., "Adaptive Control of a Variable-Impedance Ankle-Foot Orthosis to Assist Drop-Foot Gait," *IEEE Transactions on Neural Systems and Rehabilitation Engineering*, vol. 12(1), pp. 24-31, 2004.

[12] Ferris, D.P., et al., "An Improved Powered Ankle-Foot Orthosis Using Proportional Myoelectric Control," *Gait & Posture*, vol. 23, pp. 425-428, 2006.

[13] Ferris, D.P., Czerniecki, J.M., Hannaford, B., "An Ankle-Foot Orthosis Powered by Artificial Muscles," *Journal of Applied Biomechanics*, vol. 21, pp. 189-197, 2005.

SPARKy 3: Design of an Active Robotic Ankle Prosthesis with Two Actuated Degrees of Freedom Using Regenerative Kinetics.

Ryan D. Bellman, Matthew A. Holgate, Thomas G. Sugar

Abstract— **The goal of modern prosthetics is to replicate the function of the replaced limb or organ in the most capable and discreet fashion possible. However, even the most advanced, commercial, transtibial prostheses available today only passively adjust the position of the ankle during the swing phase of gait and return a portion of the user's own gravitational input. To greatly improve the quality of life of a transtibial amputee, new technologies and approaches must be used to create a cutting-edge robotic ankle prosthesis which can perform on par with, if not outperform, the equivalent able-bodied human ankle. Initial attempts by us and others have had great success in providing the natural gait power and motion through all ranges of walking speeds. A new design is presented which governs both the coronal and sagittal angles and moments of the ankle joint to potentially provide unprecedented levels of athleticism and agility among transtibial amputees.**

I. INTRODUCTION

The SPARKy Project, short for Spring Ankle with Regenerative Kinetics, began with the goal of bringing full able-bodied ankle function to transtibial amputees, particularly those injured serving in the military who wish to be able to return to active duty. The first of three planned phases culminated in a highly successful product in SPARKy 1, Fig. 1. Six months of thorough subject testing ensued, and a follow-up design was created to improve on the form and function of SPARKy 1. SPARKy 2, Fig. 2, incorporates more efficient linear transmission options using a ball screw or a roller screw, a smaller and more powerful brushless motor without the need for a gearbox and a significant overall decrease in size and weight. Both designs use the proven technology of the Robotic Tendon of Hollander[1], the elastic energy storing ability of helical springs, and an advanced carbon, composite keel. Additionally, they are both capable of permitting walking speeds in excess of 4 miles per hour, with plenty of power in reserve [2], [3]. When subject testing starts for SPARKy 2, it may even reveal to be capable of light or moderate jogging as well. Herr is developing a similar spring based ankle with motion in the sagittal plane [4].

Both ankles by Hitt et al. and Au et al. though more advanced than any technology on the market, still do not compare to the functionality of the human ankle. A more robust and agile robotic prosthesis is needed to fulfill the more demanding and athletic movements needed for an active duty soldier or an active individual. The two previous designs are limited to active motion only in the sagittal plane, but the complex movements of the human ankle also require actuation in the coronal body plane, empowering transverse body movements as well as dorso-ventral and elevational movements. The SPARKy 3 design has two degrees-of-freedom without sacrificing the size and weight precedents set by the first phase.

The initial designs for the three versions of the SPARKy ankles are shown in in Fig. 3. The size of the second version was greatly decreased using a smaller motor and shorter lever arms. SPARKy 3 added a 2nd motor and two joints without increasing overall volume.

A. Intention and Goals

SPARKy 3 has taken a unique approach to providing two degrees-of-freedom to the prosthetic ankle seeking to revolutionize powered transtibial prosthesis design. While the average amputee may not need the ability to perform agile movements, many would prefer the ability to lead a more active lifestyle without being limited by their robotic ankle; some have expressed this desire directly to us. Military amputees in particular may benefit the most from such a device, as they must

This work was supported by the U.S. Army Medical Research & Materiel Command (USAMRMC)

R. Bellman is with the Department of Mechanical and Aerospace Engineering, Arizona State University, Tempe, Arizona ryan.bellman@asu.edu

M. Holgate is with the Department of Mechanical and Aerospace Engineering, Arizona State University, Tempe, Arizona matthew.holgate@asu.edu

T. Sugar is with the Department of Engineering, Arizona State University, Polytechnic Campus, Arizona thomas.sugar@asu.edu

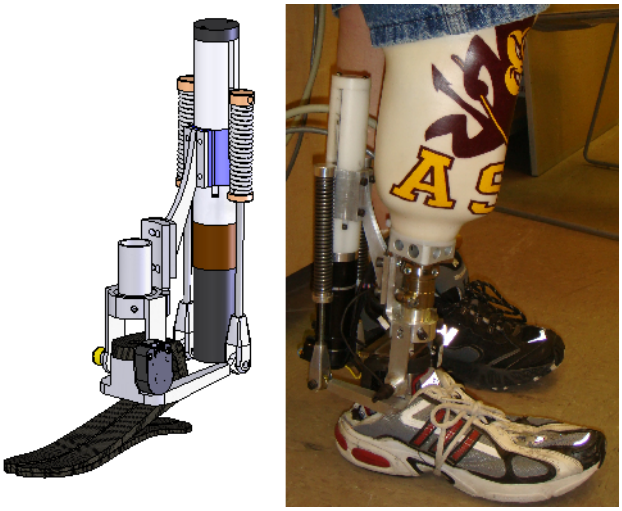

Fig. 1. The first built and tested robotic ankle prosthesis of the SPARKy Project, SPARKy 1 uses regenerative kinetics[2] to accurately and efficiently reproduce the human gait cycle. This design weighs under 2.7 kg (6 pounds) (not including the molded socket), comparable to the weight of the amputee's limb.

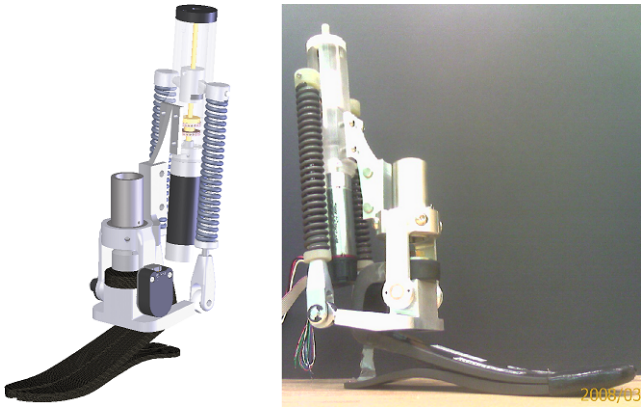

Fig. 2. The refined version of the first design evolved into SPARKy 2, incorporating a shorter lever arm, roller screw/ball screw interchangeable transmission, and the Maxon EC Powermax 30 motor[5], a high output brushless DC motor. It weighs approximately 2.0 kg (4.5 pounds) and is significantly reduced in size from its predecessor.

perform tasks such as running, jumping and passing their PT test returning to active duty service if they so desire. Our goal for the future is to allow an individual to return to active duty with increased athletic ability using two very powerful, lightweight motors.

The chief goal of this third phase of the SPARKy Project is to build a more dynamic robotic ankle without sacrificing size, weight or performance compared to the previous versions. Naturally, some compromises will have to be made to achieve these goals.

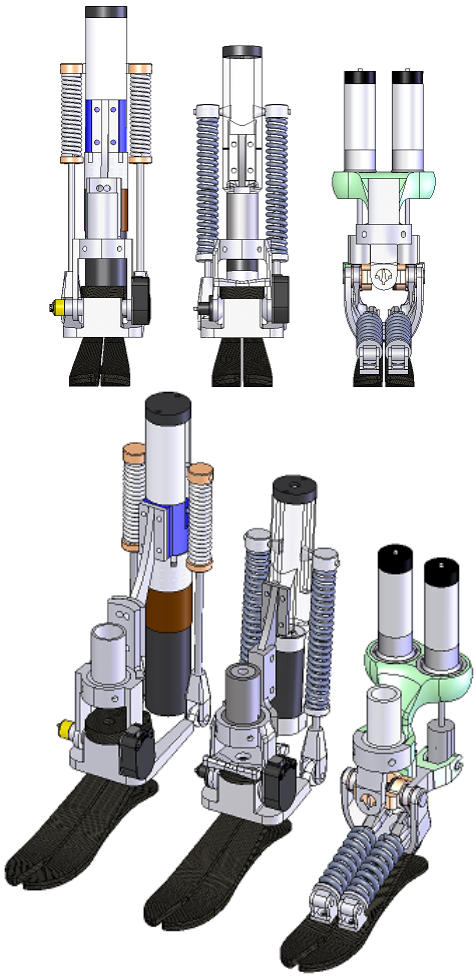

Fig. 3. The three initial designs of SPARKy 1, 2, and 3. SPARKy 2 reduces in size and weight while SPARKy 3 adds an additional degree-of-freedom.

II. Design Phase

A. *Pre-design and Sketching*

Intially, the design objectives were to achieve only running and jumping which requires two EC Powermax 30 motors to increase power capacity. The additional motor prompted investigation into adding an additional degree-of-freedom. We then focused on the idea of using both motors in unison for powered running, and controlling each individual motor to power the additional rotational degree-of-freedom.

Another desire of the design was to move the springs to a location above the keel but still in the envelope of the foot so that an unmodified shoe can still be worn over the device. This would allow for a lower profile device and remove much of mechanism from behind the leg. To additionally minimize the volume of

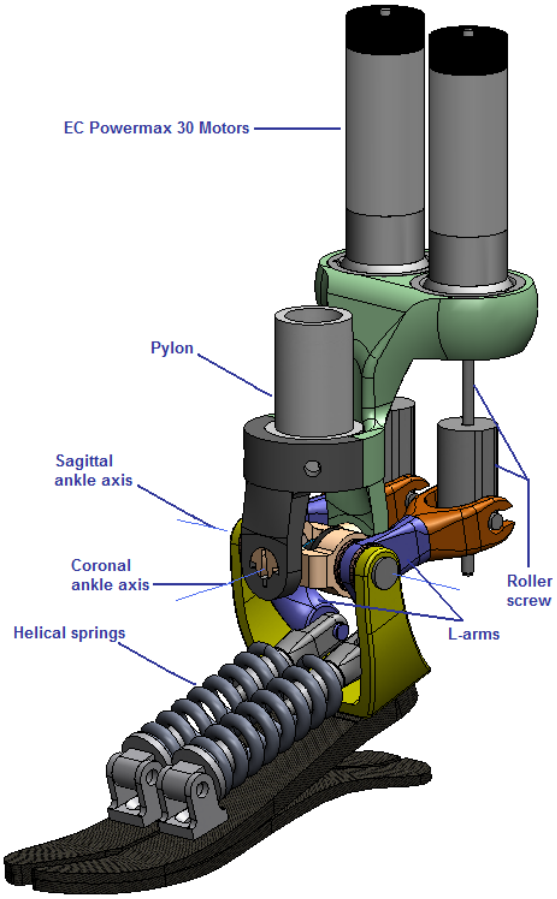

Fig. 4. SPARKy 3, the first fully actuated 2 DOF robotic prosthesis.

the design, a new low-profile foot replaces the FS3000 foot[6]. While the low-profile version of the same foot, the Pacifica FS4000[6], was considered initially, the eventual choice became Ossur's LP Vari-Flex foot [7] shown in Fig. 5. The Vari-Flex line was preferred by many users, and the design incorporates two bolts intended to hold the heel piece to the rest of the keel. These bolts proved a key factor in the decision, as they provide a perfect mounting point for the springs in our new configuration.

B. Functionality and Performance of SPARKy 3

In the primary operation of walking, the two motors work together either compressing or extending the two helical springs. For example during the stance phase, as the ankle rolls over the sagittal or primary ankle axis, the springs are extended and the motor extends the springs as well adding additional energy. During powered push-off, the motors move together releasing the energy in the springs. The combined motion has the added benefit of dividing the workload of each

Fig. 5. The low profile of the LP Vari-Flex foot by Ossur provides a low clearance keel and opens up room for a more complicated joint above it. The portion of the keel that low-profile version removes is not needed in a device with an active ankle joint, as its only purpose is to add flexibility of the ankle in a passive prosthesis.

motor. Analyzing the efficiency curve of the Maxon EC Powermax motor in Fig. 6, efficiency is greatly increased when the motor operates well below its peak capabilities. The motors will produce less heat as well, reducing the risk of failure.

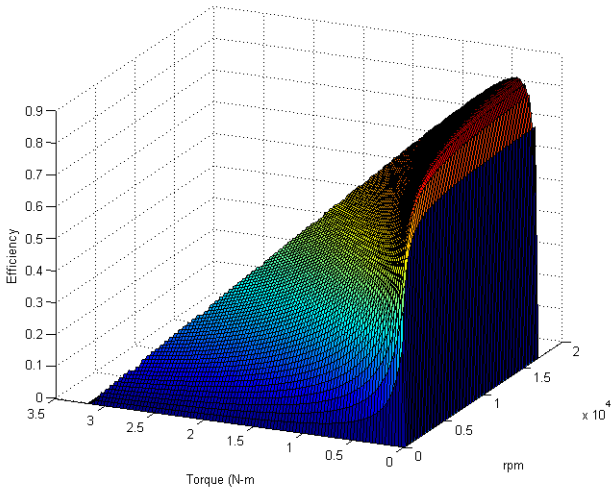

Fig. 6. The operational efficiency curve of the EC Powermax 30 motor defined by the torque load at the shaft and angular speed [3].

Additionally, the increased headroom in power of the two motors enables much more demanding activities, such as running and jumping, which do not allow as much time for energy storage from the motor as compared to walking gait thus reducing the maximum possible power amplification. Conversely, the short duration of ground contact in sprinting provides a

greater opportunity for energy storage from the impact, particularly with a higher stiffness. This principle is seen prominently in passive transtibial and transfemoral sprinting feet such as the Cheetah by Ossur. The EC Powermax 30 motor is rated at 200W of continuous output power, but is capable of much higher outputs, two to three times the continuous rating, for brief periods of time without damaging. With two such motors working together, they may be capable of 1000W or more of mechanical output power alone. Coupling this with the power amplification achievable from the robotic tendons, the SPARKy 3 design is predicted to be more than capable of producing the up to 1500W of peak output power needed for jogging and 200Nm of peak planter flexion moment for sprint starting[8], [9].

One hurdle that may yet need to be overcome is actively adjusting the stiffnesses of the springs to optimize for the significantly shorter stance phase during sprinting. Additionally, while energy savings are expected during normal walking motion compared to previous models, much greater power consumption will occur during the more agile and athletic functions of the device. Though synonymous with fatigue for the user, the device will likely require a higher capacity battery pack than is currently used on the previous models to account for the higher energy requirements, particularly for military users that are fully active and unable to recharge throughout the day.

C. CAD Design

Since SPARKy 3 was completely new, the design started around the keel. A two degrees-of-freedom joint was desired at the ankle, so a base was created to locate the plantarflexion/dorsiflexion axis, henceforth referred to as the primary axis around the biological center of rotation of a normal ankle. A couple was then designed to serve as the central part of an orthogonal custom U-joint, creating the secondary axis, for inversion and eversion. L-shaped arms, or "L-arms," were also designed to transfer the linear actuation of the actuators to the springs on the foot, using the primary axis of the ankle joint for their pivot. Due to the dimensional constraints this configuration imposes, the active lever arm through which the springs are aligned is only 4 cm as compared to the 6 cm lever arm on SPARKy 2 and the 9 cm lever arm on SPARKy 1. Because the motors are mounted 6 cm from the primary axis, an additional ratio between the motion of the actuator to the compression/extension of the springs is achieved, 1.5:1. The transmissions will be 1mm-lead roller screws similar to SPARKy 2, creating a 2/3mm effective lead between the motor and the spring. This relationship also relieves some of the load on the roller screws, as they will experience 2/3 of the force that the springs exert.

To reduce inertia effects, the mounts for the motor are fixed. Therefore, a number of additional joints are needed between the linkages to allow the device to have two degrees-of-freedom. The connection between the roller screw nut and the L-shaped arm requires two orthogonal and intersecting rotational joints to allow the motors to follow the pylon but resist the nut from turning when the roller screw shaft rotates. This was accomplished by placing a yoke reminiscent of the clevis on earlier designs on the end of the L-shaped arms and allowing it to rotate about a horizontal axis along the longer part of the arm. This interaction is shown slightly displaced from the default position to demonstrate its function in Fig. 7.

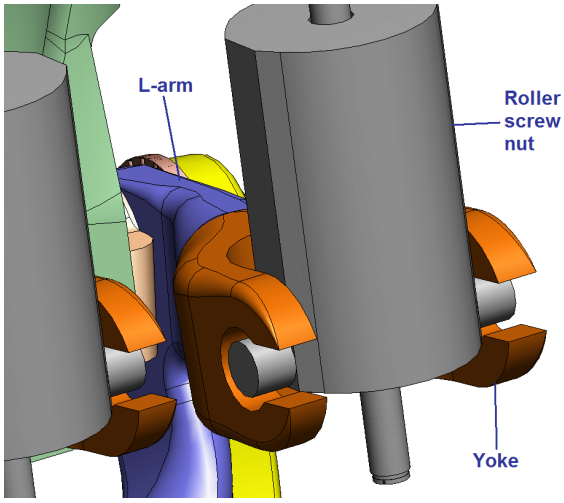

Fig. 7. The yoke swivels relative to the arm along its central axis and the roller screw wing is allowed to rotate within the yoke.

The more complex joint exists at the base of the motor mounts, as slight rotations are required to keep the roller screw shafts free from bending moments. The solution chosen involves a custom ball joint, with vertical channels on the outer race of the joint and pins on the ball to resist the torque of the motor. The ball joint was chosen due to its high load carrying characteristics without needing multiple bearings which would have cantilevered the mounts out from the pylon. The space within the ball was used to house the thrust bearings and thrust shoulder interface to reduce the size of the overall product. This portion of the design is shown from several perspectives in Fig. 8.

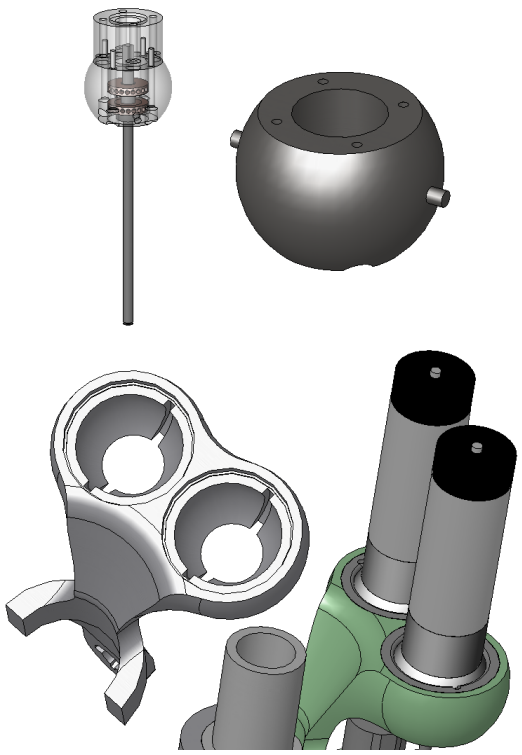

Fig. 8. The ball pieces of the ball joint interface are shown, with the actuator subassembly shown in the upper left, individual ball mount shown in the upper right, socket arm shown in the lower left, and the fully assembled ball joint interface shown in the lower right. The restricted ball joint is equivalent to two intersecting, orthogonal, rotational joints.

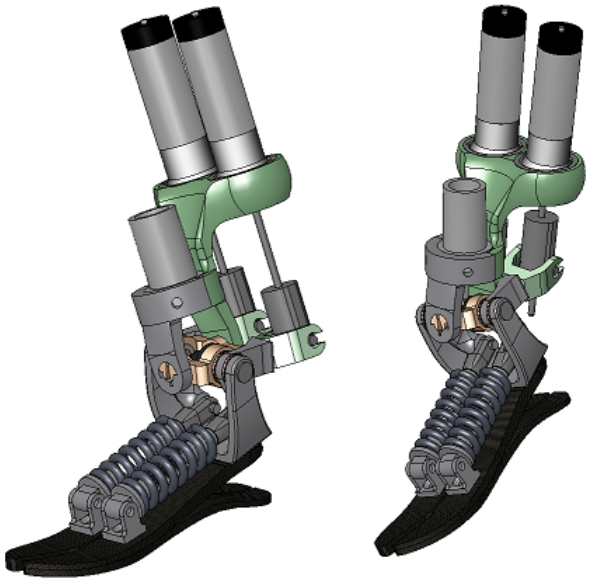

Fig. 9. The final design of SPARKy 3 in two different configurations including both coronal (frontal) and sagittal rotation from the default ankle position.

Upon completion of the design of the two additional joints, the mobility of the robotic ankle design was checked with Grubler's criterion to confirm that the foot (end effector) has two degrees-of-freedom. To perform this calculation, the mechanism had to be split into two interacting pieces, one of which operates in the plane, while the other operates in three dimensions. The current and final design of SPARKy 3 in Fig. 9 shows the device in various orientations to demonstrate its mobility. The coordination of the actuators determines the axis of motion of the device. When the actuators move in the same direction, the joint articulates about the primary axis. If the actuators move in opposing directions, the joint articulates about the secondary axis.

The geometry of the linkages means that the angular stiffness about the secondary axis is less than half that of the primary axis. Since the biological stiffness is not well documented, due to the slenderness of the human ankle, a supplemental stiffness may be necessary to increase the ankle stability about the secondary axis. It is also a safe practice to limit the motion allowed by this joint so the ankle cannot roll too far in much the same way a human ankle is rolled. The first solution was to use a hybrid torsional bearing joint manufactured by C-Flex[10]. The bearings were far too limited in both their torsional stiffness and load ratings in relation to their outside diameter and length. Instead, a custom bearing was designed. The bearing is best described visually, in Fig. 10. The torsion is achieved by adding a leaf spring between the two notches. When bent over a short length, such as the inner diameter of this bearing, a very thin leaf spring can provide a high angular stiffness, as defined by equation equation (1) from [11]. In this equation, the stiffness, K, is a function of the the modulus of elasticity of the material composing the leaf spring, E, the moment of inertia about its bending neutral axis, I, and the active length over which it is bent, L.

$$K = E * I/L \tag{1}$$

III. CONCLUSIONS AND FUTURE WORK

IV. CONCLUSIONS

Our research is focused on using springs to actively store and release energy properly during walking gait. SPARKy 1, our first regenerative ankle, was shown to store and release 16 J of energy per step. We designed and built a second device, SPARKy 2 which is lighter and more powerful using a roller screw transmission and a powerful brushless DC motor, the Maxon EC

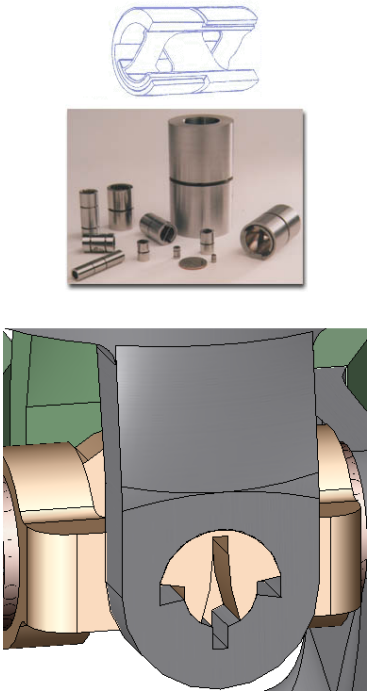

Fig. 10. The top figures are limited-motion rotational bearings manufactured by C-Flex. The bottom figure shows a custom bearing design, complete with angular limits of ± 20 degrees, torsion spring capability, and significantly higher load handling in a small and integrated package. The slot allows for the insertion of a short leaf spring to supplement the angular stiffness. Different leaf springs can be inserted for different individuals.

Powermax 30[5]. Finally, we designed and developed SPARKY 3 which is a two DOF device capable of high power for running and jumping. The design is the first to incorporate active control of both inversion and eversion as well as plantarflexion and dorsiflexion, yet will only weigh 2.1 kg (4.7 pounds) as currently designed. Combined with the power of regenerative kinetics, twin brushless DC motors, and efficient and long lasting roller screws, this device has the highest potential of returning wounded soldiers back to active duty.

V. Future Work

When SPARKy 3 is completed, subject testing will move slowly. The second degree-of-freedom and dual actuators add an element of complexity in the challenge of controlling the device. Additionally, the kinetic and kinematic data need to be analyzed for the various agile movements for which there is little or no published data. Some of this data has already been taken for basic jogging and running at various increments of speed using several rate gyros and inclinometers. Other tasks will include various lateral movements, stair and slope ascension and descension, and possibly some lateral jumping. Once these data are mated with a control system, subject testing will begin.

VI. Acknowledgments

The authors would like to acknowledge the grant that was awarded and administered by the U.S. Army Medical Research & Materiel Command (USAMRMC), under Contract Number: W81XWH-0710193. The views, opinions, findings, information and presentations made do not necessarily reflect the position of the government and no official endorsement should be made. The opinions contained in this publication are those of the authors and do not necessarily reflect those of the funding agency.

The authors would also like to thank Robotics Group Inc. and Arise Prosthetics for their participation. The authors would like to recognize Peter Rueling of the ASU Mechanical Engineering Shop for his invaluable support. Matthew Holgate, Joseph Hitt, and Kevin Hollander aided greatly in discussions about the designs.

References

[1] K. W. Hollander, R. Ilg, T. G. Sugar, and D. E. Herring, "An efficient robotic tendon for gait assistance," *Journal of Biomechanical Engineering*, vol. 128, no. 5, pp. 788–791, October 2006.

[2] J. Hitt, M. Holgate, R. Bellman, T. Sugar, and K. Hollander, "The SPARKy (Spring Ankle with Regenerative Kinetics) Project: Design and Analysis of a Robotic Transtibial Prosthesis," in *ASME International Design Engineering Technical Conference and Computers and Information in Engineering Conference*, 2007.

[3] J. K. Hitt, "A robotic transtibial prosthesis with regenerative kinetics," Ph.D. dissertation, Arizona State University, 2008.

[4] S. Au and H. Herr, "Powered ankle-foot prosthesis," in *ASME International Design Engineering Technical Conference and Computers and Information in Engineering Conference*, 2007.

[5] (2008) High precision drives and systems. Maxon Motor. [Online]. Available: http://www.maxonmotor.com

[6] (2008) Product specifications. Freedom Innovations. [Online]. Available: http://www.freedom-innovations.com

[7] (2008) Product specifications. Ossur Prosthetic Company. [Online]. Available: http://www.ossur.com/?pageid=3540

[8] M. W. Whittle, *Gait Analysis: An Introduction*, 2nd ed. Butterworth - Heineman Oxford, 1996.

[9] D. Gordon and E. Robertson. (2008) Contributions of the ankle and knee muscles to sprint starting. Sprintic Magazine. [Online]. Available: http://www.sprintic.com/articles/ankle_knee_muscles_sprint_starting

[10] (2008) Size performance and loading: Single end bearing. C-Flex Bearing Co., Inc. [Online]. Available: http://www.c-flex.com/home.html

[11] K. W. Hollander and T. G. Sugar, "Concepts for compliant actuation in wearable robotic systems," in *US-Korea Conference on Science, Technology and Entrepreneurship*, August 2004.

The SPARKy (Spring Ankle with Regenerative Kinetics) Project: Choosing a DC Motor Based Actuation Method

Matthew A. Holgate, Joseph K. Hitt, Ryan D. Bellman, Thomas G. Sugar, Kevin W. Hollander

Abstract— **The design process of a powered robotic ankle prosthesis presents many obstacles that must be overcome. To be practically implemented, such a mechanism must not only run on batteries, but sustain a long running time between recharging. Using springs to passively and actively store and supply energy to the robotic ankle, small DC motors can be optimized to perform high peak power tasks without sacrificing efficiency and net energy usage. Additional techniques are explored with the potential of substantially reducing the energy requirements as well as the size and weight of the prosthesis. The benefits of adding a unidirectional parallel spring with a Robotic Tendon are weighed and the possibility of actively varying the lever arm at which the spring force is applied is analyzed. The different actuation methods are compared to determine which methods work best in different gait regimes.**

I. INTRODUCTION

The SPARKy Project led by Arizona State University Human Machine Integration Lab with team members from Arise Prosthetics, Robotics Group, Inc. and Washington University at St. Louis is a multi-phased multi-year development effort. The project seeks to tackle several leading technical challenges that prevent the development of a truly biomimetic foot-ankle prosthetic device. This includes (1) prohibitively low power and energy density in traditional actuation schemes, and (2) development of a control methodology that translates user intent into human-like movement.

The research community has made significant improvements in prosthetic and orthotic technologies in recent years. Several prosthetic companies have produced devices that are more comfortable, provide life-like cosmeses, provide significant energy return and are now even computer controlled. New high performance composite materials and polymers have made sockets and liners more comfortable and prosthetic feet and pylons much more energy efficient. A world-class below the knee amputee sprinter using a high performance composite prosthesis can now sprint the 100 meters only one second off of the able-bodied world record [1]. Energy storage and return devices allow faster walking velocity and better terrain negotiation [2], [3], [4]. They have increased range of motion; they store and return energy; and they reduce needed energy requirements [5], [6], [7], [8], [9]. Microprocessor controller components such as the Rheo Knee use artificial intelligence to change joint angles and dampen joint motion in response to the environment and individual gait style [10]. MIT's powered foot-ankle is a microcomputer controlled prosthesis that provides power and ankle motion at normal walking speeds [11].

Hydraulic, pneumatic, direct-drive, series-elastic, electroactive polymer-based, chemical-based and many other actuation schemes are also at varying stages of research and development. Other researchers are working on wearable robot control. Embedded gait pattern control [12], EMG motion control [13][14], and state based control [15] are all in various design stages. For example, the Proprio Ankle by Ossur is a commercially available state control device that modulates ankle angle based on the environment, gait, and condition to better mimic the kinematics (opposed to both kinematics and kinetics) of the lost limb [16].

We believe that the best performance in terms of power and energy as well as system size and weight can be achieved using DC motor actuators. The purpose of this paper is to explore different methods of actuation using DC motors. The actuation methods are evaluated on their ability to give the ankle full range of motion as well as a powered push-off. The actuator must be energy efficient to extend battery life while still being able to deliver all of the necessary power for walking.

II. HUMAN GAIT

Gait is a cyclical pattern of leg and foot movement that creates locomotion[17]. To illustrate a typical pattern of gait, consider the kinematics and kinetics of a normal ankle at a self selected stride length at 1.25 m/s walking speed of an 80 kg subject, Fig. 1 and Fig. 2. Note that for different stride lengths, the curves are slightly different in magnitude and in position of peaks. The negative sign represents the physiological direction of the plantarflexing ankle, when the foot rotates downwards to push off from the ground. At the point at which the peak moment occurs, the ankle angle begins a rapid decent to its lowest overall value. The region of gait approximately between 50% and 67% of the gait cycle is known as push off. At the conclusion of push off, now considered toe off, the leg initiates swing and the foot is then positioned for the next heel strike.

The power necessary from the ankle during gait is the moment times the angular velocity of the ankle. The energy is calculated by integrating the power curve. The peak power can be up to 350 Watts and occurs during the push off portion of gait. At the beginning of gait, energy is negative as the foot resists the roll-over of the leg. During push off the energy moves sharply positive as the moment increases and

This work was supported in part by the U.S. Army Military Amputee Research Program and TATRC under Contract.

Matthew A. Holgate is with Arizona State University, Tempe, Arizona 85287 matthew.holgate@asu.edu

Joseph K. Hitt is with the US Army assigned at the Arizona State University, Tempe, Arizona 85287 joseph.hitt@asu.edu or joe.hitt@us.army.mil

Ryan D. Bellman is with Arizona State University, Tempe, Arizona 85287 ryan.bellman@asu.edu

Thomas G. Sugar is with Arizona State University, Polytechnic Campus thomas.sugar@asu.edu

Kevin W. Hollander is with Augspurger-Komm Engineering, Inc. Phoenix, Arizona 85040 kevin.hollander@asu.edu

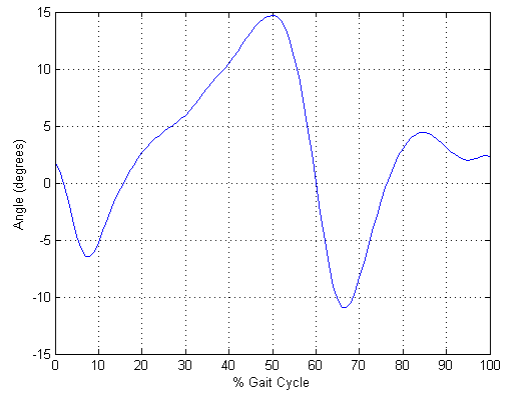

Fig. 1. The ankle angle of a normal subject walking at a self selected stride length at 1.25 m/s. 0% gait cycle corresponds to heel strike.

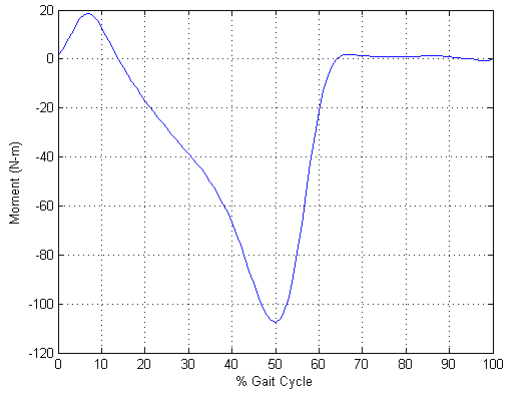

Fig. 2. The ankle moment of a normal subject walking at a self selected stride length at 1.25 m/s.

the foot propels the person. It should be noted that at self selected stride length for 1.25 m/s the net energy required is only about 10 joules per step. For slower speeds the energy becomes lower; however, for faster speeds the energy can climb to 20 joules per step or higher.

III. USING DC MOTORS

When using a DC motor actuator an important consideration is efficiency. The efficiency of a DC motor is a function of both rpm and torque. The derivation of DC motor efficiency used for this model is shown below with definitions of the symbols shown in Table I.

$$\epsilon = \frac{Trpm\frac{2\pi}{60}}{VI} \tag{1}$$

$$I = I_{nl} + \frac{T}{K_t} \tag{2}$$

$$V = \frac{rpm}{K_e} + R_m\left(I_{nl} + \frac{T}{K_t}\right) \tag{3}$$

$$\epsilon = \frac{Trpm\frac{2\pi}{60}}{\left(\frac{rpm}{K_e} + R_m\left(I_{nl} + \frac{T}{K_t}\right)\right)\left(I_{nl} + \frac{T}{K_t}\right)} \tag{4}$$

TABLE I

DEFINITIONS OF SYMBOLS SHOWN IN (1) THROUGH (4)

Symbol	Definition
ϵ	Motor Efficiency
T	Motor Torque
rpm	Revolutions per Minute
K_e	Speed Constant (rpm/Volt)
K_t	Torque Constant (N-m/Amp)
R_m	Motor Winding Resistance (Ω)
I_{nl}	Motor No-load Current (Amp)
I	Motor Current (Amp)
V	Motor Voltage (Volts)

The efficiency for a Maxon brand ECPowerMax 30 motor is plotted in Fig. 3. The highest efficiency conditions of operation are all in the low torque region of operation.

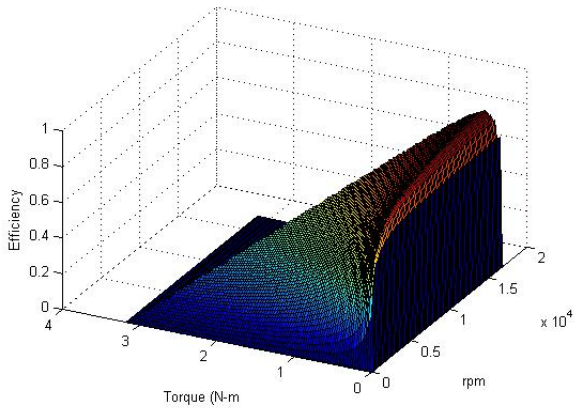

Fig. 3. Efficiency of Maxon ECPowermax30 Motor

IV. ROBOTIC TENDON

The Robotic Tendon described in [18] is a small and lightweight actuator that features an efficient DC motor used to adjust the position of helical springs using a very simple position controller. As the ankle rotates over the foot during stance phase, a lever attached to the foot pulls on the distal end of the spring. By correctly positioning the motor, which pulls on the proximal end of the spring, a desired spring deflection is obtained to store energy. A heavy, powerful motor is not needed because the Robotic Tendon stores a portion of the stance phase kinetic energy and additional motor energy within the spring. The spring releases its stored energy to provide most of the peak power required during push off. Therefore, the power requirement on the motor is significantly reduced. As described in [18], peak motor power required is 77W compared to 250W for a direct drive system in the example of a 80kg subject walking at a rate of 0.8hz. Consequently, the weight of the Robotic Tendon is just 0.95kg.

The robotic ankle consists of a spring keel for the foot; a lever arm attached to the keel; a pylon attached to the lever arm via a revolute joint; and a spring series Robotic Tendon between the pylon and the lever arm (Fig. 4). The definitions of the symbols used in Fig. 4 are shown in Table II. A defined

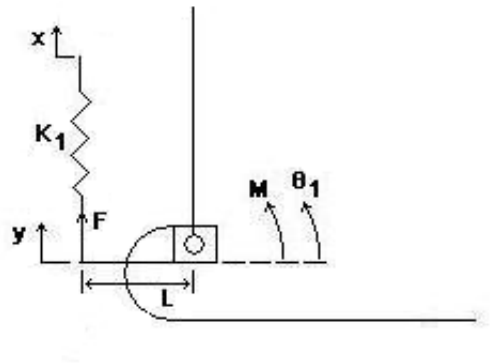

Fig. 4. Robotic Tendon Ankle Model. See Table I for definitions of symbols used. The robotic tendon nut pulls on the spring x amount, which pulls the lever arm L causing the foot to plantarflex.

TABLE II
DEFINITIONS OF SYMBOLS SHOWN IN FIG. 4

Symbol	Definition
θ_1	Lever Arm Angle (zero at horizontal)
M	Moment on the Ankle
F	Force in Spring Series Robotic Tendon
K_1	Robotic Tendon Spring Stiffness
l	Lever Arm Length
x	Robotic Tendon Spring Position
y	Lever Arm Deflection at Spring Attachment Point

moment function is given for the ankle as well as a desired angle function, shown in Fig. 1 and Fig. 2. Since the ankle has a relatively small mass and moment of inertia compared to the moments acting on it along with a limited range of motion and rotational velocity, the ankle will be assumed massless and the dynamic effects will be ignored. The motor, however, turns at a high rate and the dynamic effects can not be ignored. Using static equilibrium equations the following relationships can be developed.

$$F = K_1 (x - y) \tag{5}$$

$$y = -\theta_1 l \tag{6}$$

$$-M = lF = lK_1 (x + \theta_1 l) \tag{7}$$

$$x = -\left(\frac{M}{K_1 l} + \theta_1 l\right) \tag{8}$$

Equation (8) determines the position that the robotic tendon must follow to actuate the ankle. The spring deflection creates the ankle moment. The actuator's position is then differentiated to calculate the velocity and acceleration of the motor. Finally, the actuator velocity multiplied by the ankle moment is used to calculate power and the efficiency of the motor at every point of operation. The acceleration is used along with the inertia of the particular motor to calculate the torque necessary from the dynamic effects of the actuator. When adding the effects of inertia to the static calculations, the model matched the experimental results well.

V. PARALLEL UNIDIRECTIONAL SPRING

During the portion of the gait cycle beginning when the foot is entirely on the ground until the beginning of push off, the ankle behaves approximately like a linear spring. To illustrate this, consider the portion of Fig. 5 between points 2 and 3. Fig. 5 shows the ankle moment (Fig. 2) versus the ankle displacement angle (Fig. 1), which can be interpreted as the ankle stiffness.

If the robotic tendon series spring were chosen so that it matched the approximate linear stiffness shown in Fig. 5 between points 2 and 3 the motor would not have to move during this portion of gait. Although the motor does not need to supply any energy to the system, it still costs electrical energy because the system is backdriveable. Since the robotic tendon uses a spring in series with the motor, the moment at the ankle is transferred directly to the motor through the leadscrew transmission. If the screw were non-backdrivable, it could easily hold the load; however non-backdrivable transmissions have a large amount of friction, and thus create an inherently inefficient drive system.

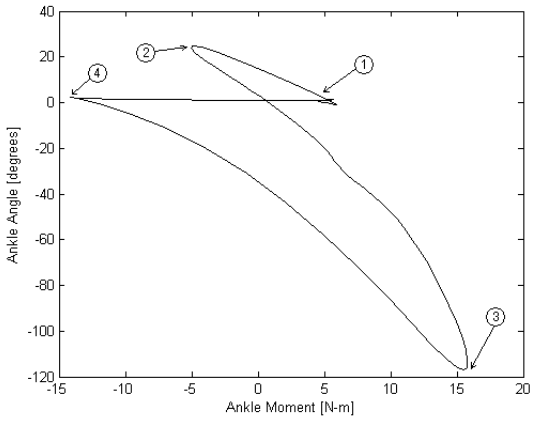

Fig. 5. Moment versus angle of the ankle for fast walking. Gait begins at point 1 with heel strike. The foot then rotates until it is flat with the ground at point 2. The tibia rolls over the ankle between points 2 and 3. Point 3 is the beginning of push off until toe off at point 4. After toe off at point 4, the foot is in swing phase until heel strike again at point 1. The slopes at different portions of gait can be thought of as the ankle stiffness and can be seen to be approximately constant during most portions.

A spring that was placed parallel to the robotic tendon could support the moment holding the load. If the parallel spring stiffness were chosen to be the ankle stiffness between points 2 and 3, then no energy would be required from the motor. However, at different speeds of walking the ankle stiffness changes. If the parallel spring stiffness was chosen to be too stiff, the motor would need to fight the spring in order to obtain the correct ankle motion. If the parallel spring was too compliant, the motor would need to add energy to the system to compensate and hold the load. A parallel spring stiffness could be fixed for a particular walking speed, and, at other speeds, the motor would need to adjust for the incorrect stiffness value.

A parallel spring is beneficial during the portion of gait shown in Fig. 5 between points 2 and 3. This portion corresponds to the portion of the stance phase when the foot dorsiflexes. When the foot plantarflexes the motor would need to fight the parallel spring and expend energy unnecessarily. To remedy this situation, the parallel spring can be configured in such a way that it is unidirectional and is only active when the foot dorsiflexes. This idea has been proven effective by researchers at MIT [11], [19]. A device with a unidirectional parallel spring can effectively lower the energy needed from the actuator especially during average and slow walking. We will show that an additional parallel spring is not beneficial for fast walking.

VI. Lever Arm

Analyzing the model for the robotic ankle shown in Fig. 4, it is reasonable to explore the possibility that the ankle could be actuated solely by changing the length of the lever arm. Solving equation (7) for l instead of x yields the following.

$$l = \frac{-xK_1 \pm \sqrt{(xK_1)^2 - 4\theta_1 K_1 M}}{2\theta_1 K_1} \tag{9}$$

If x is thought of as a constant offset on the spring, then the Robotic Tendon will not have to move during the entire gait cycle. (A non back-driveable transmission is a good choice for this design scenario.) It is apparent from the square root term in equation (9) that only certain values of x will work. For this idea to be feasible the following relationship must always be true.

$$(xK_1)^2 - 4\theta_1 K_1 M > 0 \tag{10}$$

The rest position of the spring must be set at a large offset value, larger than the range of the ankle moment so that equation (10) holds.

Another way to study this problem is to analyze the ankle as a simple torsional spring. By dividing the moment by the angle at every point of the gait cycle, a stiffness will be calculated. These values are shown in Fig. 6. It is obvious that many of the values are not attainable. However, by moving the resting equilibrium position of the spring, the stiffness values become realizable. This is modeled by adding a constant to the angle so that the resulting stiffness function is continuous. This is illustrated in Fig. 7. As the constant becomes larger, the effect of the ankle motion becomes smaller and the stiffness converges to the moment divided by the constant angle. It should be noticed that the stiffness values are both positive and negative. This can be realized by a lever arm that can go past a zero length and effectively reverse the direction of the moment.

By preloading the spring, the resting position is altered. The lever arm length needed at each point along the gait cycle is calculated using equation (9). The force on the spring is calculated using equation (5).

If a design is utilized that moves the position of the attachment point of the spring along the lever arm, the force on an actuator motor that adjusts the lever arm will be the product of the force on the spring and the sine of the angle of the lever arm. The power will therefore be the product of that force and the linear velocity along the lever arm. The motor would have to supply a large holding force unless a drive link that was not backdrivable was utilized.

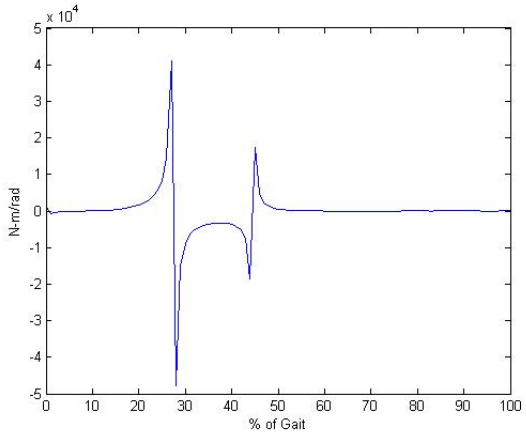

Fig. 6. Moment divided by angle. The ankle moment is divided by the ankle angle to determine a stiffness value at every point along the gait cycle. It is obvious that many of the stiffness values are not realizable.

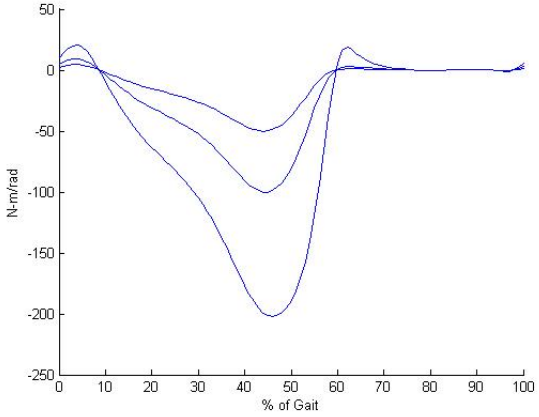

Fig. 7. Moment divided by angle with an additional positive constant offset. The moment is divided by the ankle angle with an additional constant angle to determine a stiffness value at every point along the gait cycle. Each curve represents a different constant offset. The stiffness converges to the inverse of the constant times the moment because as the constant becomes greater, the effect of the ankle motion becomes smaller.

An adjustable lever arm actuator has some advantages over the Robotic Tendon actuator. Analyzing fast and slow walking, the total energy consumed by the lever arm actuator is lower by 10-15% as compared to the Robotic Tendon. The energy is lower than the Robotic Tendon because the torque and rpm that is required is in a more efficient region of the motor shown in Fig. 3.

A pure lever arm actuator seems beneficial in simulations and theory, but in practice it creates many implementation problems. The system requires a preload of the spring of at least 3cm in practical cases. While this is a small deflection, the spring rates required are on the order of 50,000 N/m. A 3cm deflection creates a considerable force. During the entire gait cycle, forces can approach 2200 N on the spring. A structure could be designed to withstand this loading, and it would operate correctly while the foot was in contact with

the ground. Although during swing phase, the foot is not in contact with the ground and the force in the spring is still very high causing the foot to be difficult to control during this period of the gait cycle.

VII. COMBINING A ROBOTIC TENDON WITH LEVER ARM ACTUATION

While using a robotic lever arm alone might not be possible from a design standpoint, it is advantageous when it comes to saving energy. The energy savings occur because the motor is operating in a more efficient manner. Because there there can be an advantage gained by using a robotic lever arm, it seems reasonable to try and combine the actuated lever arm with a Robotic Tendon to increase the efficiency of the total system.

Analyzing Fig. 3, it is obvious that there is an area of operation over which the efficiency is very high, on the order of 85 to 90%. It is seen that the high efficiency peak roughly follows a straight line located with a low but constant torque and through almost all angular velocities. By adjusting the lever arm length, the gear ratio for the Robotic Tendon can be adjusted.

Since the moment at the ankle joint is transferred to the Robotic Tendon through a lever arm, the torque seen by the motor is proportional to the lever arm length. If the lever arm length is changed in proportion to the moment, the torque at the motor can be kept constant. The constant torque at the motor can be chosen to reside on the high efficiency peak of Fig. 3. As a result the efficiency of the Robotic Tendon motor is extremely high, almost always above 87%. Moreover, the energy required from the Robotic Tendon is reduced at all speeds as well.

However, the energy reduction does not come free; energy must be added due to the lever arm motor. Since the lever arm length must change when the lever is under load, there are times when it must compress the spring in order to shorten or lengthen the lever arm. In fact, almost all of the lever arm movements compress the spring. This is not necessarily a disadvantage, since the energy is stored in the spring and subsequently released. However, the efficiency of the lever arm actuation motor must also be taken into account. Even though lever arm actuation allows the main motor to work at very high efficiency, the lever arm motor efficiency is relatively low and the energy advantage for this motor is poor.

It can be observed that since the lever arm would need to change proportionally to ankle moment, this could possibly be accomplished by a clever mechanism. As seen in [20], using a carbon fiber keel can be beneficial in the design of a prosthetic ankle. This adds the benefit of a member of the structure which deflects proportionally to the ankle moment. A flexible keel could be linked in such a way that a deflection actuates the lever arm length eliminating the lever arm actuation motor.

VIII. PEAK POWER AND ENERGY

In this section, the peak power and energy will be analyzed for a Robotic Tendon with addition of a unidirectional parallel spring. Both spring stiffness values will be varied to determine power and energy surface plots.

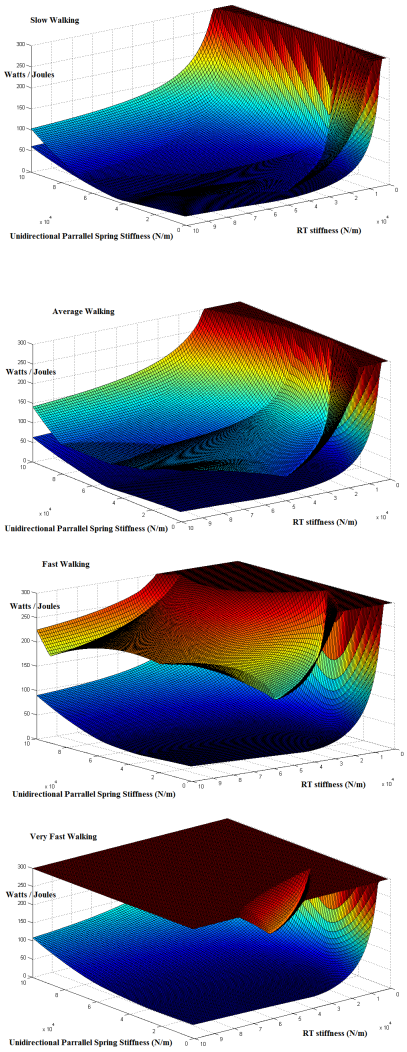

Fig. 8. Peak power and energy for different walking speeds for different stiffness values for the Robotic Tendon series spring and an additional parallel unidirectional spring. Note that values are cut off at 300 to preserve scale. The top surface is the peak power that the actuator needs to provide; the bottom surface is the energy that the actuator needs to provide. Note that most of the peak powers are above the range available for small DC motors.

As discussed in previous sections, using a unidirectional parallel spring can reduce the amount of energy needed from the actuator. This is highly beneficial for walking, especially walking at the speed for which the unidirectional spring is tuned. However, for faster walking speeds, for which the parallel spring is not tuned, additional energy from the actuator is required. Without a parallel spring the motor must hold position, but only if the series stiffness is chosen to be equal to the ankle stiffness between points 2 and 3 of Fig. 5. If a more compliant actuator series spring is chosen, the motor can continuously stretch the spring and add energy to the system as it is pulling, not simply holding position.

At slow walking speeds, the energy with a properly tuned unidirectional spring with a very stiff Robotic Tendon stiffness is slightly lower than the energy necessary for a Robotic Tendon alone. At faster speeds, however, the advantage is lost

for a constant stiffness parallel spring. At very fast walking, the lowest peak power and energy usage occurs with the correct choice of a Robotic Tendon spring.

The main advantage of the Robotic Tendon is its ability to reduce the peak power required from the motor. For average walking speeds the peak power is not as important as energy, the peak power only needs to be reduced by a small amount to stay below the maximum power of the motor. However, for fast walking speeds the peak power must be reduced if a single DC motor is used. SPARKy has shown through testing that the Robotic Tendon consistently reduces power by at least a factor of 4.5. For example, at 3 mph, the robotic tendon inputs 60 Watts peak power, but SPARKy supplies the user 260 Watts of peak power [21]. If jogging is to be achieved, peak power reduction is even more important.

Reducing peak power also increases the maximum amount of energy that the motor can provide to the ankle. Since the motor can add energy to the spring for a longer period, more energy can be released during push off. The ankle receives energy stored in the series spring during the stance phase along with additional power from the motor. With a parallel unidirectional spring the spring supplies some of the push off energy, but the motor must directly supply the remainder of the energy, which is a large portion of the energy.

IX. CONCLUSIONS

Various DC motor based actuation methods for a prosthetic ankle were investigated. These actuation methods include the Robotic Tendon alone, adding a unidirectional parallel spring to the ankle with a Robotic Tendon, controlling the length of a lever arm connected to a preloaded spring, and combining the Robotic Tendon with a robotic lever arm.

Controlling the lever arm length connected to a preloaded spring turns out to be a very efficient design, but, due to impracticalities, cannot be chosen as a realizable actuator for SPARKy. While combining lever arm actuation with the Robotic Tendon allows the system to operate extremely efficiently, the lever arm motor operates with poor efficiency and the total energy is higher than with the Robotic Tendon alone.

The Robotic Tendon operates efficiently and does not require high energy and reduces peak power by up to a factor of 6. This allows good battery life at all speeds and the ability to shrink the size of the necessary motor.

Adding a unidirectional parallel spring to the ankle can reduce the energy consumed by the Robotic Tendon by supporting its load during part of the gait cycle. This can reduce the energy slightly if properly tuned, but power amplification is lost (must choose a very high stiffness) and the motor cannot support high energy fast walking and running.

Considering performance characteristics of the motor and desired operating ranges that include walking and slow running, we have chosen the Robotic Tendon as the preferred actuation method for SPARKy.

X. ACKNOWLEDGMENTS

The authors would like to thank Greg Sawicki from the University of Michigan for providing us with invaluable gait data.

REFERENCES

[1] [Online]. Website, URL www.mshirley.com, Marlon Shirley's Personal Site, 2006.

[2] J. Casillas, V. Dulieu, and M. Cohen, "Bioenergetic comparison of a new energy-storing foot and SACH foot in traumatic below knee vascular amputations," Archives of Physical Medicine and Rehabilitation, vol. 76, pp. 39-44, 1995.

[3] S. Rao, L. Boyd, and S. Mulroy, "Segment velocities in normal and transtibial amputees: prosthetic design implications," IEEE Transactions on Rehabilitation Engineering, vol. 6, pp. 219 -226, 1998.

[4] L. Torburn, J. Perry, E. Ayyappa, and S. Shanfield, "Below-knee amputee gait with dynamic elastic response prosthetic feet: a pilot study," Journal of Rehabilitation Research and Development, vol. 27, pp. 369 -384, 1990.

[5] M Linden et la, "A methodology for studying the effects of various types of prosthetic feet on the biomechanics of trans-femoral amputee gait," Journal of Biomechanics, vol 32, pp. 877-889, 1999.

[6] J. Lehmann, R. Price, S. Boswell-Bessette, et al, "Comprehensive analysis of energy storing prosthetic feet: Flex-Foot and Seattle Foot versus standard SACH foot," Archives of Physical Medicine and Rehabilitation, vol. 74, pp. 1225-1231, 1993.

[7] P. MacFarlane, D. Nielsen, D. Shurr, and K. Meier, "Gait comparisons for below-knee amputees using a Flex-Foot versus a conventional prosthetic foot," Journal of Prosthetics and Orthotics, vol. 3, pp. 150 -161, 1991.

[8] K. Postema, H. Hermens, J. de Vries, et al., "Energy storage and release of prosthetic feet. Part 1: Biomechanical analysis related to user benefits," Prosthetics and Orthotics International, vol. 21, pp. 17-27, 1997.

[9] K. Postema, H. Hermens, J. de Vries, et al., "Energy storage and release of prosthetic feet. Part 2: Subjective ratings of 2 energy storing and 2 conventional feet, user choice of foot and deciding factor," Prosthetics and Orthotics International, vol. 21, pp. 28 -34, 1997.

[10] [Online]. Website. Rheo Knee Technical Manual, Ossur Orthopaedic Products and Services Company URL http://www.ossur.com , 2006.

[11] S. Au, "Powered Ankle-Foot Prosthesis," ASME International Design Engineering Technical Conference & Computers and Information in Engineering Conference, Las Vegas, NV, 2007.

[12] J. Ward, J. Hitt, T. Sugar, and K. Bharadwaj. "Dynamic Pace Controller for the Robotic Gait Trainer," ASME International Design Engineering Technical Conference & Computers and Information in Engineering Conference, Philadelphia, PA, 2006.

[13] S. Au, P. Bonato, and H. Herr, "An EMG-position controlled system for an active ankle-foot prosthesis: An initial experimental study," IEEE International Conference on Rehabilitation Robotics, 2005.

[14] D. P. Ferris, K. E. Gordon, G. S. Sawicki, A. Peethambaran, "An improved powered ankle-foot orthosis using proportional myoelectric control," Gait & Posture, 2005.

[15] I. Pappas, M. Popovic, T. Keller, V. Dietz, and M. Morari. ""A Reliable Gait Phase Detection System,"" IEEE Transaction on Neural Systems and Rehabilitation Engineering, vol. 9, pp. 113-125, 2001.

[16] [Online]. Website. Proprio Technical Manual, Ossur Orthopaedic Products and Services Company URL http://www.ossur.com, 2006.

[17] M. W. Whittle. Gait Analysis: An Introduction, 2 ed. Oxford: Butterworth-Heinemann, 1996.

[18] K. W. Hollander, R. Ilg, T. G. Sugar, and D. Herring. "An Efficient Robotic Tendon for Gait Assistance," *ASME Journal of Biomechanical Engineering*, vol 128(5), pp. 788-791, October 2006.

[19] Au, S. K., Weber. J., and Herr, H., "Biomechanical design of a powered ankle-foot prosthesis," Proc. IEEE Int. Conf. On Rehabilitation Robotics, Noordwijk, The Netherlands, pp. 298-303, June 2007.

[20] J. Hitt, R. Bellman, M. Holgate, T. Sugar, K. Hollander, "The SPARKy (Spring Ankle With Regenerative kinetics)Project: Design and Analysis of a Robotic Transtibial Prosthesis With Regenerative Kinetics," Proceedings of the ASME 2007 International Design Engineering Technical Conferences & Computers and Information in Engineering Conference, Las Vegas, Nevada, 2007.

[21] Joseph K. Hitt, Matthew Holgate, Thomas G. Sugar, Ryan Bellman, Alex Boehler and Kevin W. Hollander, "The SPARKy (Spring Ankle With Regenerative kinetics)Project: Power and Energy Considerations of a Robotic Transtibial Prosthesis," Submitted to Proc. IEEE Int. Conf. On Rehabilitation Robotics 2008.

Robotic Transtibial Prosthesis with Biomechanical Energy Regeneration

Abstract

Purpose: By applying "regenerative kinetics" the project seeks to develop a new generation of powered prostheses based on lightweight, uniquely-tuned, energy-storing elastic elements in series with optimal actuator systems that will significantly reduce the peak power requirement of the motor and the total system energy requirement while providing the amputee 100% of required "push-off" power and ankle sagittal plane range-of-motion comparable to able-bodied gait.

Design/methodology/approach: This paper presents the design, the power and energy efficiency analyses, and the results of a 5 month trial with one trans-tibial amputee subject as part of the first phase of the SPARKy (Spring Ankle with Regenerative Kinetics) project.

Findings: The data will show that by leveraging uniquely tuned springs and transmission mechanisms, motor power is easily amplified more than 4 fold and the electric energy requirement is cut in half compared with traditional approaches.

Originality/value: This paper describes an energy efficient, powered transtibial prosthesis currently unavailable commercially. Motor power and energy requirements are reduced with use of a unique design that employs regenerative kinetics.

Keywords: Powered Prostheses, Efficient Mechanisms, Kinetics, Rehabilitation Robots, Amputees

Paper type: Research paper

1. Introduction

There have been significant improvements in prosthetic and orthotic technologies in recent years. Several prosthetic companies have produced devices that are more comfortable, provide life-like cosmeses, provide significant energy return, and are now even computer controlled. Energy storage and return devices allow faster walking velocity and better terrain negotiation (Casillas, 1995; Rao, 1998; Torburn, 1990). They have increased range of motion; they store and return energy; and they reduce the needed metabolic requirements (Linden, 1999; Lehmann, 1993; MacFarlane, 1991; Postema, 1997).

Hydraulic, pneumatic, motor/gearbox, series-elastic, electroactive polymer-based, chemical-based and many other actuation schemes are also at varying stages of research and development (Klute et al, 2002; Au and Herr, 2008; Sawicki and Ferris, 2008; Fite and Goldfarb, 2008; Versluys et al, 2008). Other researchers are working on wearable robot control. From the highly publicized neuro-controlled bionic arm (Popular Magazine, 2005) to embedded gait

pattern control (Ward and Hitt, 2006), EMG motion control (Au and Bonato, 2005; Ferris and Gordon, 2005) and state based control (Pappas, 2001), they are all producing positive results. The Proprio Ankle by Ossur is the first commercially available motorized and computer controlled ankle device that modulates ankle angle based on the environment, gait, and conditions to better mimic the kinematics of the lost limb, however, without the functionality to actively generate power (Ossur Online, 2009).

2. Power and Energy Density

A portable, daily-use powered prosthesis such as SPARKy requires both high power to weight ratio (power density) and energy to weight ratio (energy density) in an actuator (Hitt, 2008). Without these limitations, one could take, for example, a RE75 DC Motor from Maxon Precision Motors, Inc. rated for 250 W continuous power to provide the 250 W peak power required in human gait (80 kg subject at 0.8 Hz walking) (Hollander, 2006). But this motor in combination with a gearbox in a traditional approach would weigh 6-7 kg, which exceeds the weight of a typical biological below knee limb. Providing the idealized 36 Joules of energy per step (Hollander, 2006) also becomes an issue because one must consider the efficiency of the motor, gearbox and other transmission mechanisms, friction and inertia, and the consumption of energy by the sensors and electronics. Just the mechanism inefficiency alone can double the energy requirement. For example, a DC motor with an average efficiency of 70%, connected to a ball screw at 90% and a gearbox at 80% multiply to produce a 50% efficiency actuation system. This would suggest a doubling of the energy input requirement to 72 Joules/step to provide the necessary 36 Joules/step at the output end. This is an optimistic estimate because this does not include several other factors such as: the energy consumed to counter motor/actuator inertia, which our tests show, is considerable in a highly cyclical gait pattern where the motor rapidly changes direction several times per step, friction in the mechanism or energy required by the microprocessor, sensors, motor controller, etc., Fig 1. One can easily see that actual energy requirement could grow to three or four fold of the idealized number of 36 Joules/step in a traditional approach and consequently increasing the battery requirement proportionately to non-portable levels. Also under these circumstances, slow running which may quadruple the peak power requirement as compared to normal walking (1000 W for heel to toe running as compared to 250 W for walking) would send power and energy density requirements beyond what can be achieved.

3. Motor Power Requirement

SPARKy utilizes the Robotic Tendon (Hollander, 2006) actuator to minimize the peak motor power requirement by correctly positioning a uniquely tuned helical spring so that the spring provides most of the peak power required for gait. The Robotic Tendon is a small and lightweight actuator that features a low energy motor that is used to adjust the position of the helical spring using a very simple position controller. The work differs from the series elastic actuator because the proximal side of the spring is controlled using position feedback, and the distal side of the spring is not controlled. Fig. 2 illustrates how the desired spring deflection and consequently via Hooke's Law the desired force and ankle moment is achieved using a spring. As the ankle rotates over the foot during the stance phase, a lever position profile as shown in Fig. 2 is obtained. By correctly positioning the motor, a desired spring deflection as shown in the shaded area of Fig. 2 is obtained. A heavy, powerful, impedance controlled motor is not needed because the Robotic Tendon stores a portion of the stance phase kinetic energy and additional motor energy within the spring. The spring releases its stored energy to provide most of the peak power required during "push off." Therefore, the power requirement on the motor is significantly reduced. As described in (Hollander, 2006), peak motor power required is 77 W

compared to 250 W for a motor/gearbox system in the 80 kg subject at a 0.8 Hz example. Consequently, the weight of the Robotic Tendon, at just 0.95 kg, is 7 times less than an equivalent direct drive motor and gearbox system that is required to provide the necessary peak power. In other words, the Robotic Tendon achieves a power density that in essence is 7 times greater than a traditional approach. Fig. 3, in comparison with Fig. 1, illustrates the addition of regenerative power and energy made possible with the spring in series with the motor.

4. Motor Energy Requirement

SPARKy increases energy density of the actuation system by using the spring, which is almost 100% efficient, to provide most of the energy. Additionally, ideal motor energy requirement, as determined by the integration of the power curves, is reduced from nearly 36 Joules in the 250 W peak power case to 21 Joules per step in the 77 W peak power case described above (80 kg subject walking at 0.8 Hz.) This significantly reduces the energy input burden of the motor and it allows the much more efficient helical spring to store and release energy.

Another significant aspect of energy density is motor efficiency. The RE40 DC Motor by Maxon, Inc. (Maxon Online, 2009) currently used in the Phase I SPARKy is one of the most efficient motors commercially available for this application. However, its rated efficiency of 90% is only achieved at a very small range of motor torque and angular velocity - near 7000 rpm at 0.1 Nm. Below 2000 rpm and above 0.2 Nm, motor efficiency quickly drops below 50%. The motor efficiency 3D plot is shown in Fig. 4 as a function of motor torque and motor rpm.

Fig. 4 shows that there is a narrow range of motor efficiency above 70%. Once the motor slows below 2000 rpm or motor torque exceeds 0.2 Nm, the motor efficiency degrades exponentially. Therefore, the motor should be properly matched with an appropriate gearing mechanism that maintains high motor speed and low torque.

On SPARKy Phase I, a 4.3 gear ratio gearbox from Maxon rated at 90% efficiency, ¼ inch-16 turns/inch ACME 4 start lead screw and an adjustable length lever are used to achieve high motor efficiency. A lead screw was selected over other rotation to translation mechanisms such as a ball screw or a roller screw for several reasons. A ball screw is highly efficient because of its rolling contact but is limited in terms of the dynamic load rating. Roller screws are also very efficient and they have high dynamic load ratings but the price can be prohibitive.

The efficiency of a typical lead screw is low compared to the other transmission mechanisms mentioned above. By using a small diameter lead screw with a proportionately large lead, one can achieve a lead angle that allows for maximum efficiency. By selecting a lubricated steel lead screw and bronze nut, one can achieve a coefficient of friction below 0.1. The efficiency of our lead screw is 0.7 as determined by the method outlined in (Hollander, 2006).

5. SPARKy Design

5.1 Mechanical Design

The mechanical design of SPARKy has presented several obstacles that needed to be overcome to maximize the energy output without limiting the comfort, capability and safety of the robot. Fig. 5 shows two perspectives of the modeled prosthetic ankle. A new parallel two spring Robotic Tendon is attached to a custom aluminum pylon and to a commercial FS3000 Keel from Freedom Innovations via a lever. The three sensors that provide closed loop

feedback are not shown in these illustrations. The computer and electronics are packaged in a portable 5" x 7" case worn at the hip for the current phase of SPARKy I.

The mechanical design includes two safety features. First, the threading of the lead screw is removed at both ends to allow for free spin of the lead screw nut so that the ankle cannot over extend in plantarflexion or dorsiflexion directions. Additionally, the ankle joint is mechanically limited to normal ankle joint ranges as a secondary counter-measure for over-extension.

5.2 Electronics, Sensors and Computing

SPARKy is controlled in real time using Real Time Workshop and Simulink from Mathworks. The Simulink model is compiled on to the embedded target PC running the xPC Target Operating System. An encoder at the motor, an encoder at the ankle joint and an optical switch embedded at the heel provides the necessary sensor feedback. Advantech's 650MHZ PC-104 with 512MB on board memory is selected to run the system. A multifunctional I/O board from Sensoray Co., Model 526, which is connected to the PC104 via an ISA bus, controls a RE-40 Maxon DC motor with encoder feedback. Future prototypes will make use of a computing system fully contained in the prosthesis.

Two safety features are designed into the electronics of the prototype. A handheld dead man's switch must remain engaged to maintain power to the motor. An emergency stop is incorporated into the power system that an investigator can use to cut the power to the entire system.

5.3. Control

Together with power and energy density, computer control of prostheses remains a significant challenge. Efforts towards control methodology that produce biologically realistic movement in prostheses and orthoses began in the early 1960s with work such as the Belgrade Hand. However, even after a half century of work, achieving human like control is proving to be very difficult. Work by Au et al and Ferris et al in EMG position control (Au, 2005; Ferris, 2005) and by Pappas et al in state based control (Pappas, 2001) seems promising because of its simplicity. Sugar's effort to reduce the control problem using compliant simple force control (Sugar, 2002) is a key finding towards simplifying control methodology and served as our starting point with the Robotic Tendon.

The SPARKy controller, as described in (Hitt, 2007; Hitt, 2007), has a predetermined gait pattern, which is based on able-bodied gait data (Whittle, 1996) and kinetic analysis (Hollander, 2006), expressed as a time-based function embedded in the controller, which drives the motor controller and thus the system. Gait is initiated at heel strike with activation of an optical switch embedded in the heel. As the user initiates gait, the motor drives the lead screw nut through a pattern predetermined for each subject with closed loop feedback. The ankle, however, is not forced to follow the specific pattern because the compliant spring is between the motor and user, safely absorbing environmental irregularities such as a rock under foot or user errors. This inherent compliance not only provides for a safer interface, but allows for a much simpler control scheme because high-bandwidth, high-precision force control is not required.

6. SPARKy Modeling

Ankle joint angle and moment data used in the simulation are from able-bodied data generated by inverse dynamics of motion capture and force plate test data and published by Whittle (Whittle, 1996). The remaining kinetic and kinematic analysis is derived using a quasi-static approach. MATLAB simulation of the models showed that a power amplification of up to 6

may be possible. Presented here is one of those models selected for SPARKy Phase 1 for its simplicity and robustness in terms of mechanical design and control. Simulation of this model showed that a power amplification of more than three is possible while maintaining gait kinematics and kinetics similar to able-bodied persons.

In the simple series model, the keel and the Robotic Tendon springs are in series; therefore, the moment in the keel is equal to the moment in the Robotic Tendon. Motor position is controlled so that the moment of the Robotic Tendon matches that of the able-bodied moment data, Equation (1). K_a is the keel stiffness in N/m; K_s is the spring stiffness in N/m; B is the radius of the keel deflection in meters; d is the moment arm due to the keel deflection in meters; and *l* is the lever length in meters. See Fig. 6. Note that the derivation applies small angle approximations.

$$M_A(t) = M_{keel}(t) = M_{RT}(t) \qquad (1)$$

$$where:$$

$$M_A \quad from\ published \quad AB\ data \quad [24]$$

$$M_{keel}(t) = -K_a B d \varphi(t)$$

$$M_{RT}(t) = K_s (x(t) - l\theta(t)) l$$

Solving Equation (1) for motor position, *x(t)*, determines the expression in Equation (2):

$$x(t) = l\theta(t) - \frac{K_a B d}{K_s l}\varphi(t) \qquad (2)$$

The assumed force in the Robotic Tendon is given by Equation (3):

$$F(t) = \frac{M_A(t)}{l} \qquad (3)$$

The ideal power generated by the motor to move to position *x(t)* is given by the product of the force and velocity in the tendon, Equation (4):

$$P_m(t) = F(t)\ \frac{dx(t)}{dt}$$

$$\Rightarrow P_m(t) = \frac{M_A(t)}{l}\left[l\frac{d\theta(t)}{dt} - \frac{K_a B d}{K_s l}\frac{d\varphi(t)}{dt} \right] \qquad (4)$$

The expression in Equation (4) represents the power required by the motor to generate the desired moment and ankle angle of able-bodied gait (Whittle, 1996) given that the spring provides the majority of the required peak power.

Optimization of Equation (4) varying keel stiffness, K_a, and spring stiffness, K_s, showed that a minimum peak motor power profile is achieved by varying K_s as seen in Figure 7. This figure is a surface plot of the peak power at a given spring and keel stiffness. It shows that a spring stiffness of 32000 N/m is optimal in terms of minimum peak motor power. At this spring stiffness, the peak motor power is at its lowest value of 80 W. As the tendon spring becomes rigid, required motor power reaches that of a rigid system. As the tendon spring stiffness reaches zero, required motor power becomes asymptotically large.

The results are significant because it shows that SPARKy with use of a keel and Robotic Tendon can achieve significant kinetic advantages. With an input power of 80 W from the motor, this simulation illustrates that SPARKy, with use of springs, can deliver the required 260 W of peak gait power, which is a power amplification of 3.25. Fig. 8, generated from the simulation, shows the motor, gait and keel power profiles. Notice that the motor power peaks at 80 W and the gait power peaks at 260 W. The keel power profile is not additive because the system is in series. However, the keel power profile is similar to what is found in literature describing the power of energy storage and return (ESAR) keels.

This series model achieves 100% of the required peak gait power with less than a third of the peak input power (motor power) by harnessing the energy storage potential of springs. In addition, because the system's joint motion is controlled only by the counter-moments of the tendon spring and keel, kinematics of the system is almost identical to the desired able-bodied gait, see Fig. 9. This total motion of SPARKy provides its user with kinematics similar to able-bodied gait kinematics representing a significant improvement from today's state of the art.

7. SPARKy Testing

SPARKy Phase I device was tested on a single transtibial amputee male subject for a period of five months walking on a treadmill. Embedded sensor data such as motor and ankle encoder information were recorded at varying walking speeds with varying spring stiffness, lever lengths, and loading condition. In addition direct measurements of motor current and voltage information were recorded. This information was used to determine the ankle kinematics and kinetics of the user on the SPARKy device. Fig. 10 is a picture of a transtibial amputee test subject, 80 kg, walking over level ground using SPARKy.

Fig. 11 shows the desired ankle position as modeled previously and the actual ankle position measured using the ankle encoder. Testing shows that SPARKy achieves full ankle sagittal plane range of motion. The ankle position is quite accurate and smooth even though the distal side of the spring is not controlled.

Fig. 12 shows the desired motor and gait output powers determined from our simple series model described earlier. Using measured spring deflection to determine the force at the spring and ankle and motor encoder information to determine the velocity at the motor and at the ankle, motor and output powers are determined using the product of force and velocity. The measured powers are in very good agreement with the modeled powers. Fig. 13 shows the measured motor power and the measured output power for a series of 9 gait cycles of our subject walking at 1.3 m/s (3 mph). The power amplification is consistently above 4.5 (Peak Output Power/Peak Motor Power). The motor only outputs 60 W peak but SPARKy with the use of springs delivers 270 W of peak power to the user. Fig. 14 shows the measured power from the motor and spring. Notice that the spring provides the majority of the power required during push-off.

Electric power used by the motor is determined using the direct measurement of current and voltage to the motor, Fig. 15. Integration of the electric power provides the energy input requirement for SPARKy at 1.3 m/s (3mph) as 43 J/s or 43W. Output power is the product of the measured ankle velocity and force. Integration of the output power provides the energy output by SPARKy at 1.3 m/s (3mph) as 35 J/s or 35W. Therefore, the system efficiency in terms of average power in and out is 0.81. This level of efficiency is possible because majority of the work is done by the springs. We have similar data and results with the subject walking at 0.5, 1, 1.3 and 1.8 m/s.

8. Conclusion

We presented in this paper the design, analysis and testing of the Phase I SPARKy. We showed that this approach gains kinetic advantages by leveraging elastic energy potential in uniquely tuned helical springs. As the tibia rotates over the stance foot ankle during walking gait, we position the spring to maximize elastic energy storage. We presented the synergistic benefits of the Robotic Tendon in terms of motor efficiency and power and energy reductions. We presented test data to show that we achieved a power amplification of 4.5 consistently with the motor providing a peak of 60 W and the spring providing the remaining 210 W so that the user had a peak of 270 W at push off while walking at 1.3 m/s (3mph). We showed that the system is 81% efficient in terms of the average electric power in to the motor (43 W) and average mechanical power out to the user (35 W). This level of efficiency is possible because the springs perform the majority of the work. We also show that SPARKy can provide 100% of the push-off power required in walking gait while maintaining gait kinematics similar to able-bodied gait.

9. References

Au S., Berniker, M., Herr, H. (2008), “Powered ankle-foot prosthesis to assist level-ground and stair-descent gaits,” Neural Networks, vo. 21, pp. 654–666.

Au, S., P. Bonato, and H. Herr (2005), "An EMG-position controlled system for an active ankle-foot prosthesis: An initial experimental study," IEEE International Conference on Rehabilitation Robotics.

Casillas, J., V. Dulieu, and M. Cohen (1995), “Bioenergetic comparison of a new energy-storing foot and SACH foot in traumatic below knee vascular amputations,” Archives of Physical Medicine and Rehabilitation, vol. 76, pp. 39–44.

Ferris, D., K. E. Gordon, G. S. Sawicki, A. Peethambaran (2005), "An improved powered ankle–foot orthosis using proportional myoelectric control," Gait & Posture.

Fite, K., Thomas J. Withrow, Xiangrong Shen, Keith W. Wait,Jason E. Mitchell, and Michael Goldfarb (2008), “A Gas-Actuated Anthropomorphic Prosthesis for Transhumeral Amputees,” IEEE Transactions on Robotics, VOL. 24, NO. 1.

Hitt, J., A. Oymagil, T. Sugar, et al. (2007), “Dynamically Controlled Ankle-Foot Orthosis with Regenerative Kinetics: Incrementally Attaining User Portability,” Proceedings of the 2007 IEEE International Conference on Robotics and Automation, Roma, Italy.

Hitt, J., M. Holgate, R. Bellman, T. Sugar, K. Hollander (2007), “The SPARKy (Spring Ankle with Regenerative Kinetics) Project : Design and Analysis of a Robotic Transtibial Prosthesis, ” ASME International Design Engineering Technical Conference & Computers and Information in Engineering Conference, Las Vegas, NV.

Hitt, J. (2008), “Design and Control of a Robotic Transtibial Prosthesis with Regenerative Kinetics,” PhD Dissertation, Arizona State University, Tempe, Arizona.

Hollander, K., Robert Ilg, T. G. Sugar, and D. E. Herring (2006), “An Efficient Robotic Tendon for Gait Assistance,” ASME Journal of Biomechanical Engineering, vol 128(5), pp. 788-791.

Hollander. K., and T. G. Sugar (2006), “Design of Lightweight Lead Screw Actuators for Wearable Robotic Applications,” ASME Journal of Mechanical Design, vol. 128(3), pp. 644-648.
Klute, G., Czerniecki, J., and Hannaford, B. (2002), “Artificial muscles: actuators for biorobotic systems,: The International Journal of Robotics Research, vol. 21. No. 4, pp. 295-309.
Lehmann, J., R. Price, S. Boswell-Bessette, et al (1993), “Comprehensive analysis of energy storing prosthetic feet: Flex-Foot and Seattle Foot versus standard SACH foot,” Archives of Physical Medicine and Rehabilitation, vol. 74, pp. 1225–1231.
Linden et al (1999), “A methodology for studying the effects of various types of prosthetic feet on the biomechanics of trans-femoral amputee gait,” Journal of Biomechanics, vol 32, pp. 877-889.
MacFarlane, P., D. Nielsen, D. Shurr, and K. Meier (1991), “Gait comparisons for below-knee amputees using a Flex-Foot versus a conventional prosthetic foot,” Journal of Prosthetics and Orthotics, vol. 3, pp. 150 –161.
[Online]. (2009) Website. Proprio Technical Manual, Ossur Orthopaedic Products and Services Company URL http://www.ossur.com.
[Online]. (2009) Website. RE40 Motor Specifications, Maxon Motor, Inc., URL http://www.maxonmotor.com.
Pappas, I., M. Popovic, T. Keller, V. Dietz, and M. Morari (2001), "A Reliable Gait Phase Detection System,"" IEEE Transaction on Neural Systems and Rehabilitation Engineering, vol. 9, pp. 113-125.
Popular Magazine Article (2005), “Neuro-Controlled Bionic Army,” November Issue.
Postema, K., H. Hermens, J. de Vries, et al. (1997), “Energy storage and release of prosthetic feet. Part 1: Biomechanical analysis related to user benefits,” Prosthetics and Orthotics International, vol. 21, pp. 17–27.
Postema,K., H. Hermens, J. de Vries, et al. (1997), “Energy storage and release of prosthetic feet. Part 2: Subjective ratings of 2 energy storing and 2 conventional feet, user choice of foot and deciding factor,” Prosthetics and Orthotics International, vol. 21, pp. 28 –34.
Rao, S., L. Boyd, and S. Mulroy (1998), “Segment velocities in normal and transtibial amputees: prosthetic design implications,” IEEE Transactions on Rehabilitation Engineering, vol. 6, pp. 219 –226.
Sawicki, G., and Daniel P. Ferris (2008), “Mechanics and energetics of level walking with powered ankle exoskeletons,” The Journal of Experimental Biology 211, 1402-1413.
Sugar, T. (2002), "A Novel Selective Compliant Actuator," Mechatronics Journal, vol. 12, pp. 1157-1171.
Torburn, L., J. Perry, E. Ayyappa, and S. Shanfield (1990), “Below-knee amputee gait with dynamic elastic response prosthetic feet: a pilot study,” Journal of Rehabilitation Research and Development, vol. 27, pp. 369 –384.
Versluys, R., Desomer, A., Gerlinde, L., et al (2008), “A biomechantronical transtibial prosthesis powered by pleated pneumatic artificial muscles,” International Journal of Modelling, Identification and Control, vol. 4, No. 4, pp394-405.
Ward, J., J. Hitt, T. Sugar, and K. Bharadwaj (2006), “Dynamic Pace Controller for the Robotic Gait Trainer,” ASME International Design Engineering Technical Conference & Computers and Information in Engineering Conference, Philadelphia, PA.
Whittle, M. (1996), Gait Analysis: An Introduction, 2 ed. Oxford: Butterworth-Heinemann.

Fig. 1. This diagram illustrates the flow of power and energy from the battery to the user. Significant amount of energy is lost due to inefficiency in the mechanisms, motor, inertia, friction, etc. Proper selection and design can drastically improve overall system efficiency. The system efficiency is defined as average output power to the user/average input power from the battery.

Fig. 2. Desired spring deflection, shaded area, is achieved by controlling the motor position and capitalizing on the cyclical nature of gait. As the tibia rotates over the stance foot, the lever extends the springs. Simultaneously, the motor extends the spring in the opposite direction to achieve the desired spring deflection and via Hooke's Law the forces required to generate the required ankle moment for walking.

Fig. 3. This diagram illustrates the flow of energy from the battery to the user for the Robotic Tendon model. Even though significant amount of energy is lost due to inefficiency in the mechanisms, motor, inertia, friction, etc., the spring and the regenerative energy that it harnesses is nearly 100% efficient and accounts for the main share of the output energy. This method also allows for a smaller motor, battery and transmission system.

Fig. 4. 3D plot of the RE40 motor efficiency as a function of motor torque (Nm) and motor angular velocity (rpm). Notice that the highest efficiency of 90% is only achieved at a narrow range of torque and angular velocity. Operating the RE40 at speeds lower than 2000 rpm or torque above 0.2 Nm will significantly degrade the motor efficiency. Illustrated in the figure are two points on the mesh.

Fig. 5. Isometric and side views of current design as modeled in Solid Works. The RE40 motor coupled with the robotic tendon provide a dynamic moment about the ankle joint.

Fig. 6. A 2 degrees-of-freedom model with a seismic excitation representing the motor excitation, a torsional spring for the keel and a helical spring between the lever and the motor is shown. The moment due to the keel is a function of $\varphi(t)$ and the moment due to the spring is a function of $x(t)$-$l\Theta(t)$. The moment at the ankle is from published information determined using inverse dynamics of motion capture and force plate test data as published in Whittle, 1992.

Fig. 7. A surface plot of the peak power from Equation (4) varying K_a and K_s. Notice that at a spring stiffness of 32,000 N/m, the minimum peak motor power of 80 W is achieved. Keel stiffness does not greatly influence the design in this optimization.

Fig. 8. The power profiles for able-bodied gait (system output power). required motor power and power from the keel. (From simulations.)

Fig. 9. The ankle joint angle, the keel deflection angle, and the sum of both angles. (From simulations.)

Fig. 10. A picture of a transtibial amputee using SPARKy overground.

Fig. 11. The desired ankle movement and the actual ankle movement for one walking gait cycle. The subject was walking at 1 m/s (2.2 mph) on a treadmill.

Fig. 12. The ideal output and motor power determined by the simple series model, vs. the measured output and motor power.

Fig. 13. The measured motor power and output power for 9 gait cycles. The power amplification is consistently above 4.5 (270W peak/60W peak). (Our test data has shown amplifications of 6 and 8 are possible.)

Fig. 14. The motor power and the spring power sum to the output power. The spring provides the majority of the push-off power required in gait.

Fig. 15. The dashed line is the electric power input as determined by the measured current and voltage to the motor. The solid line is the same output power shown in Fig. 13.